NOVA SCHOOL OF SCIENCE & TECHNOLOGY

DEPARTAMENTO DE CIÊNCIAS E ENGENHARIA DO AMBIENTE

DAVID EMANUEL PINTO GASPAR

Licenciado em Ciências de Engenharia do Ambiente

ELECTRODIALYTIC RECOVERY OF TUNGSTEN AND COBALT FROM AN INDUSTRIAL RESIDUE

PRELIMINARY ASSESSMENT

MESTRADO EM ENGENHARIA DO AMBIENTE

Universidade NOVA de Lisboa
novembro 2021

DEPARTAMENTO DE CIÊNCIAS E ENGENHARIA DO AMBIENTE

ELECTRODIALYTIC RECOVERY OF TUNGSTEN AND COBALT FROM AN INDUSTRIAL RESIDUE

PRELIMINARY ASSESSMENT

DAVID EMANUEL PINTO GASPAR
Licenciado em Ciências de Engenharia do Ambiente

Orientadora: Paula Alexandra Rodrigues e Araújo Guedes,
Investigadora,
CENSE, Universidade NOVA de Lisboa

Coorientadora: Alexandra de Jesus Branco Ribeiro,
Professora Associada com Agregação
Universidade NOVA de Lisboa

Júri:

Presidente: Maria Teresa Calvão Rodrigues, Professora Auxiliar,
Universidade NOVA de Lisboa

Arguente: Ana Rita Lourinho Ferreira, Investigadora,
Technical University of Denmark

Vogal: Paula Alexandra Rodrigues e Araújo Guedes,
Investigadora,
CENSE, Universidade NOVA de Lisboa

MESTRADO EM ENGENHARIA DO AMBIENTE

Universidade NOVA de Lisboa
Novembro 2021

Electrodialytic recovery of tungsten and cobalt from an industrial residue – preliminary assessment

To my grandma Rita Maria,

who left us during this journey

ACKNOWLEDGEMENTS

I would like to express my gratitude to some people, who were important not only during this work but in many moments of my life:

First, to Professor Alexandra B. Ribeiro, my co-advisor, for arousing my interest in raw materials and for showing me the potential of an environmental engineer to work in this area. Thanks for materializing this in the wonderful opportunity to collaborate with CENSE and RESOLUTION Lab on this challenging topic. This work has received funding from the European Union's Horizon 2020 research and innovation program under the Marie Skłodowska-Curie grant agreement No. 778045. This work is anchored by the RESOLUTION LAB, a laboratory at NOVA School of Science and Technology.

To Doctor Paula Guedes, my advisor, for her unconditional help, availability, immense knowledge, and (a lot of) patience she presented me during these months of hard but profitable work. Thanks for the perfect combination of empathy and professionalism naturally established since the beginning, which made scientific discussions pleasant.

Additionally, to RESOLUTION Lab members, especially to Doctor Eduardo Mateus, for providing everything I needed in this work. To my laboratory colleagues, for welcoming me with open arms, and providing a good working environment as well as the help they kindly provided when I needed it. To Lorenzo Gianni, my Italian lab partner, who shared this "tungsten carbide recovery adventure" with me.

To my *alma mater*, FCT NOVA, for these five years, that it became my home and, that between highs and lows, where I grew up not only as a student but also as a man. To all the professors who marked me, especially to Professor Graça Martinho, for all the research projects in which I collaborated with her team (waste@NOVA), and that allowed me to put the acquired knowledge into practice.

To the friends that university gave me, and I will definitely take for life. I want to mention some names, under penalty of forgetting someone: Beatriz Reigada, Beatriz Soares, Catarina Pereira, Filipa Caeiro, Francisco Marques-Pinto, João Polaco Santos, João Vacas and Ruben Cruz. To most of you, I hope this work will be an inspiration to yours. I also thank my friends outside the university, who have always been with me.

To all my family, especially to my parents, Lara and José, firstly for my existence, but above all for efforts they made so I would never give up and constantly fight for my goals; to my grandparents: Rita and Amâncio, for the essential role they had in my education, and for still being present in my heart; Maria do Rosário and Manuel, that fortunately continue by my side, for always encouraging me. I would also want to express a grateful word to my uncle Rui and to the memory of my great-uncle Nicolau.

Last but not the least, I would like to thank to all people who for any reason are not mentioned, but have contributed over these years, directly or indirectly, to make this possible.

"The man is the engineer of his own destiny"

ABSTRACT

Critical raw materials (CRMs) have a significant importance for key sectors in the European economy. This importance will continue to grow due to the Green Deal, as the sustainable transition to carbon neutrality by 2050 is settled in modern technologies and renewable energies, which are closely linked to a need for many raw materials.

Europe is very highly dependent on imports of most of the raw materials needed by European industries, with a set of CRMs presenting a high level of concentration in particular countries, some of them geopolitically unstable. For this reason, the supply chains security depends largely on efficient management of resources throughout the lifecycle and the commitment to recycling using secondary resources, such as industrial residues. Investing in CRMs' recycling processes and their sustainability is essential to maintain the supply chains.

The present work is the first attempt to study the application of the electrodialytic (ED) process for recovery of two CRMs, tungsten (W) and cobalt (Co), from tungsten carbide (WC-Co) scrap powder resultant from end-of-life cutting tools. ED process consists of the application of a low-level electric current, in the presence of cation and/or anion exchange membranes, which promote the separation between compartments.

In this specific work, acid desorption of W and Co from the matrix was carried out, followed by electromigration and electrodialysis. Eight experiments were carried out during 24h, using ED cells with three (3C) and two (2C) compartments to perform three assessments: the best electrolyte, the best solid:liquid ratio, and the best current intensity. The WC-Co matrix was placed in the central cell compartment in the 3C setup and directly in the anode in a 2C cell. The results show that the 2C cell setup with NaCl 0.02 M as catholyte and citric acid 0.4 M as anolyte, a solid:liquid ratio 1:25, and an initial current intensity of 200 mA presented the highest W (2194 mg; 99.6% of total W solubilized) and Co (558 mg; 81.3% of total Co solubilized) recovery. However, the current intensity was not completely optimized yet and needs further investigation.

This dissertation will contribute to guide future experimental work to optimize the ED conditions for W and Co recovery.

Keywords: Electrodialytic process, critical raw materials, recycling, tungsten carbide, tungsten, cobalt, recovery

RESUMO

As matérias-primas críticas (CRMs) possuem uma importância significativa para setores-chave da economia europeia. Essa importância vai continuar a aumentar com o Pacto Ecológico Europeu, uma vez que a transição sustentável para a neutralidade carbónica em 2050 está assente em tecnologias modernas e energias renováveis, intimamente ligadas a uma grande necessidade de um vasto número de matérias-primas.

A Europa depende largamente das importações da maioria das matérias-primas necessárias às suas indústrias, materiais esses altamente concentrados num conjunto de países específicos, alguns deles geopoliticamente instáveis. Por esse motivo, a segurança das cadeias de abastecimento depende em grande parte da gestão eficiente dos recursos ao longo do seu ciclo de vida e do compromisso com a reciclagem, recorrendo a fontes secundárias como resíduos industriais. Investir nestes processos, bem como a garantir a sua sustentabilidade, é fundamental para assegurar a manutenção das cadeias de abastecimento.

O presente trabalho consiste na primeira tentativa de estudar a aplicação do processo eletrodialítico (ED) para recuperação de duas matérias-primas críticas, tungsténio (W) e cobalto (Co), a partir de um pó de carbeto de tungsténio (WC-Co) macerado, resultante de ferramentas de corte em fim-de-vida. O processo ED consiste na aplicação de uma corrente elétrica de baixa intensidade, na presença de membranas de troca catiónica e/ou aniónica, que promovem a separação entre compartimentos.

Neste trabalho específico, foi realizada uma dessorção ácida de W e Co da matriz sólida, seguida de eletromigração e eletrodiálise. Cada uma de oito experiências foi realizada durante 24h, utilizando células ED com três (3C) e dois (2C) compartimentos com três objetivos: obter o melhor eletrólito, o melhor rácio sólido:líquido e a melhor intensidade de corrente. A matriz de WC-Co foi colocada no compartimento central da célula 3C e diretamente no ânodo na célula 2C. Os resultados mostram que a configuração da célula 2C com NaCl 0.02 M como catolito e ácido cítrico 0.4 M como anolito, um rácio sólido:líquido de 1:25 e uma intensidade de corrente inicial de 200 mA apresentou a maior recuperação de W (2194 mg; 99.6% do total de W solubilizado) e Co (558 mg; 81.3% do total de Co solubilizado). No entanto, a intensidade da corrente ainda não foi completamente otimizada, necessitando de mais investigação.

Esta dissertação contribuirá para futuros trabalhos experimentais com vista a otimizar as condições do processo ED para a recuperação de W e Co.

Palavras-chave: Processo eletrodialítico, matérias-primas críticas, reciclagem, carbeto de tungsténio, tungsténio, cobalto, recuperação

TABLE OF CONTENTS

LIST OF FIGURES

LIST OF TABLES

ABBREVIATIONS AND SYMBOLS

AEM – Anion exchange membrane
AN – Anolyte
APT – Ammonium paratungstate
CAT – Catholyte
CEM – Cation exchange membrane
CRM – Critical raw material
DC – Direct current
EC – European Commission
ED – Electrodialytic
EK – Electrokinetic
HCit – Citric acid
ICP-AES - Inductively Coupled Plasma-Atomic Emission Spectrometry
ITIA – International Tungsten Industry Association
LIB – Lithium-ion batteries
LCA – Life cycle assessment
LP – Liquid phase
MC – Mechano-chemical
MMO – Mixed metal oxide
USGS – United States Geological Survey
WC – Tungsten carbide
WC-Co – Tungsten carbide(-cobalt)

1. INTRODUCTION

Modern society is highly reliant on technology, whose development is dependent on an increasing range of raw materials. The benefits of technologies are conditioned by raw materials supply, so their risks become of great relevance for the European industry, leading to the emergence of many policy initiatives and research projects to deal with the growing concerns about the sustainability and security of raw materials supply. The focus on critical metals comes from many features related to supply security, such as integrated supply chains, similar production processes, and the possibility of recycling from end-of-life products. However, there are other raw materials (non-critical and/or non-metallic) with the same importance and risks associated with their supply (Lovik *et al.*, 2018).

The critical raw materials (CRMs) supply can be provided from primary sources (essentially mining industry) or secondary sources (through recycling methods). Europe imports most of the raw materials needed by European industries, so its security depends largely on efficient management of resources throughout the lifecycle and the commitment to recycling CRMs from secondary resources. To that extent, substitution and recycling are considered risk-reducing measures for establishing the EU list of CRMs (EC, 2018).

Two of these CRMs are tungsten (W) and cobalt (Co), which have been identified since 2011 as being among the list of the CRMs vital to the EU industries. Tungsten and Co are also two of CRMs with higher recycling rates (42% for W and 35% for Co). They remained on this list in 2014, 2017 and 2020, due to their economic importance and risk of supply disruption (EC, 2018; Rizzo *et al.*, 2020). Tungsten is a stable transition metal with a wide range of uses, such as cemented carbides, mill products, alloys, and steels (Cuesta-Lopez, 2017) while cobalt is a ferromagnetic metal, used especially for heat-resistant and magnetic alloys (Slack *et al.*, 2017).

Cemented carbide, which represents by far the largest consumption of tungsten worldwide, consists of a carbide cutting tool manufactured with a mixture of fine particles of W and Co (the binder that holds tungsten carbide together), with a wide range of variations in carbide grain size and the carbide:binder ratio (Lunk & Hartl, 2019). Cobalt is a remarkable binding metal and is generally used to produce machining tools due to its excellent wear resistance, mechanical hardness, and toughness (Seo & Kim, 2016). According to the

distribution of cutting tools in the global market in 2018 by the cutting method and workpiece material, it is shown that milling, turning, and drilling are the most used processes in primary machining operations (almost 87% of the total tooling market) (Rizzo *et al.*, 2020).

Tungsten carbide (WC-Co) scraps have been considered as an important secondary source of W and Co metals. Recycling of these carbides requires specialized techniques, such as hydro or pyrometallurgical or a combination of them; thermal oxidation, followed by acid/alkali leaching or reduction by hydrogen to produce W powder; or even direct leaching of WC scrap in concentrated acid/alkali solutions. Electrochemical techniques have emerged as an attractive method for recycling WC-Co waste as it is a single-step dissolution process that consumes very low energy and provides very pure outcomes compared to the other recycling methods (Katiyar & Randhawa, 2014). In addition to the type of electrolytes used, the anode passivation during anodic dissolution is still a great concern, which can reduce the effectiveness of the process, limiting the electrodissolution. Therefore, improving anodic dissolution is considered the most challenging step in the electrochemical recycling of WC waste from a productivity point of view (Katiyar & Randhawa, 2020).

Instead of anodic dissolution, the present work tested a different electrochemical treatment – the electrodialytic (ED) process – through an acidic media to recover W and Co from WC-Co scrap powder resultant from cutting tools. ED is one of the most relevant membrane methods to separate ionic species from an aqueous solution or other uncharged matrices, induced by an electric field (Oliveira *et al.*, 2019; Villen-Guzman *et al.*, 2019). ED process is applied to remove contaminants from porous matrices, which has been shown to be effective in removing heavy metals from solid matrices, with removal rates above 80% and low energy consumption (Pedersen *et al.*, 2017).

The specific aim of this thesis is to develop an electrochemically based technology to recover W and Co from tungsten carbide (WC-Co) waste. Some experimental tests were carried out at a laboratory scale, using 3- and 2- compartment modular ED cells. The preliminary results obtained on this treatment, such as several operational parameters (adjuvants, solid:liquid ratio, and current intensity), will contribute to future developments of this work area.

1.1. Study objective and research

The present dissertation aims to answer the following questions:

A) What are the best acid conditions for W and Co desorption?
B) What are the best ED process parameters for W and Co recovery from WC-Co scrap?
C) Is the ED process a viable technology for W and Co recovery from WC-Co scrap?

To find answers to these questions, experimental tests were carried out at RESOLUTION Lab. The sample was WC-Co scrap powder provided from ReCarb (Boston, MA, USA).

To answer question A), desorption tests were carried out using 0.5 g of WC-Co scrap powder. Different mineral acids (HNO_3 and HCl) and organic acids (Citric acid and oxalic acid) were tested (replicates), contemplated with desorption as a function of time.

To answer questions B) and C), the sample was submitted to the ED process in order to assess the W and Co recovery rates, using as a starting point the results of answer A). Eight experiments were carried out during 24h under different conditions, such as the use of adjuvants, the number of cell compartments and sample placement, the solid:liquid ratio, and the current intensity.

All answers were supported through the W and Co quantification in the liquid samples by Inductively Coupled Plasma-Atomic Emission Spectrometry (ICP-AES).

1.2. Dissertation structure

The present work is organized into eight chapters:

1. Introduction – work scope and relevance, main objectives and structure;
2. Literature review – description of the central theme, relevant terminology, and previous work developed;
3. Materials and methods – description of materials used, characterization analysis, identification, and data treatment methods;
4. Results and discussion - presentation of results, hypotheses formulation and their discussion;
5. Conclusions – main outcomes;
6. Future developments

   References

A. Appendix

2. LITERATURE REVIEW

2.1. Critical Raw Materials and Circular Economy

The European Green Deal is the new EU strategy for economic growth adopted by the European Commission (EC) in 2019, arising as an integral part of actions related to the implementation of the United Nation's 2030 Agenda and Sustainable Development Goals (SDG). One of the most important tasks of this plan is the mobilization of the industry for a clean and circular economy model, as the EU announced in 2014. The circular economy assumes a transition from a linear to a circular model, in which waste can become a valuable resource. Therefore, it is recommended to use raw materials more efficiently and improve its recycling (Smol *et al.*, 2020).

Raw materials are crucial in the production of a wide range of goods and applications that are used in daily life. The EU industry is largely dependent on imports for many raw materials, which means that the EU has high exposure to vulnerabilities through all stages of the supply chain in various sectors. They are an essential building block of the EU's growth and competitiveness, and their relevance will increase to accompany the global energy transition. Raw materials with the greatest economic importance and high supply risk are called critical raw materials (CRMs) (EC, 2018; EC, 2020b).

The demand for CRMs between 2010 and 2030 is expected to double due to the acceleration of technological innovations and the rapid growth of emerging economies. The climate ambition of the Green Deal reinforces the link to CRMs, since the aim to no net emissions of greenhouse gases by 2050 will require electrification efforts and the diversification of sources of energy supply which in turn requires a huge increase in raw materials (EC, 2020c). For those reasons, the Commission developed an integrated strategy called European Raw Materials Initiative, which started in 2008. Its aims focus on the growing concern for security and improving access to raw materials for the EU economy. One of the biggest actions of this Initiative was to create a list of CRMs at the EU level (EC, 2018; EC, 2020b).

This assessment at the EU level focuses on a wide range of raw materials and started in 2011, being updated every three years. The fourth and most recent list of CRMs for the EU was adopted in 2020 and includes 30 CRMs, present in Table 2.1. Nonetheless, even if the raw material is not considered critical, their availability and importance for the EU economy should not be neglected. Moreover, the availability of new data and possible evolutions in EU and international markets may influence the list in the future (EC, 2020a). The US Geological Survey has a similar list, actualized in the Final List of Critical Minerals in 2018 (Table 2.2).

Table 2.1. List of Critical Raw Materials for the EU in 2020 (adapted from European Commission, 2020). Materials that are not present in the US Geological Survey list are highlighted.

2020 Critical Raw Materials		
Antimony	Germanium	Platinum Group Metals
Baryte	Hafnium	Phosphate rock
Bauxite	Heavy Rare Earth Elements	Phosphorus
Beryllium	Indium	Scandium
Bismuth	Light Rare Earth Elements	Silicon metal
Borate	Lithium	Strontium
Cobalt	Magnesium	Tantalum
Coking Coal	Natural Graphite	Titanium
Fluorspar	Natural Rubber	Tungsten
Gallium	Niobium	Vanadium

Table 2.2. Final List of Critical Minerals for US Geological Survey (adapted from US Geological Survey, 2018). Materials that are not present in the EU CRMs list are highlighted.

Final List of Critical Minerals 2018		
Aluminium (bauxite)	Graphite (natural)	Rubidium
Antimony	Hafnium	Scandium
Arsenic	Helium	Strontium
Barite	Indium	Tantalum
Beryllium	Lithium	Tellurium
Bismuth	Magnesium	Tin
Cesium	Manganese	Titanium
Chromium	Niobium	Tungsten
Cobalt	Platinum Group Metals	Uranium
Fluorspar	Potash	Vanadium
Gallium	Rare Earth Elements Group	Zirconium
Germanium	Rhenium	

These commodities classified as "critical minerals" have a vulnerable supply chain and an essential function in the manufacturing of a product, which absence would have several consequences for the economy or national security (US Geological Survey, 2018). Although most critical minerals for the US Geological Survey (Table 2.2) are the same as the European Commission list (Table 2.1), some different materials can still be found, and are highlighted in both tables. This is attributed to the different economies, industries, or resources. There are also some differences of terminology or combination between the two lists, e.g. barite/baryte (US and EN English) or Rare Earth Elements Group on the US list which corresponds to Heavy REE and Light REE on the EU list.

China is largely the principal supplier of CRMs to the EU, but several other countries represent important shares of the EU supply for specific CRMs (Figure 2.1), such as the USA (beryllium), Turkey (borate), Chile (lithium), or South Africa (platinum group metals). The EU also relies on single EU companies for its supply of hafnium and strontium (EC, 2020b). Some differences between the 2018 and 2020 reports on the EU's CRMs needs can exemplify why it leads the EU to constantly monitor its actual supply to get a more realistic picture of the European supply of raw materials assessed.

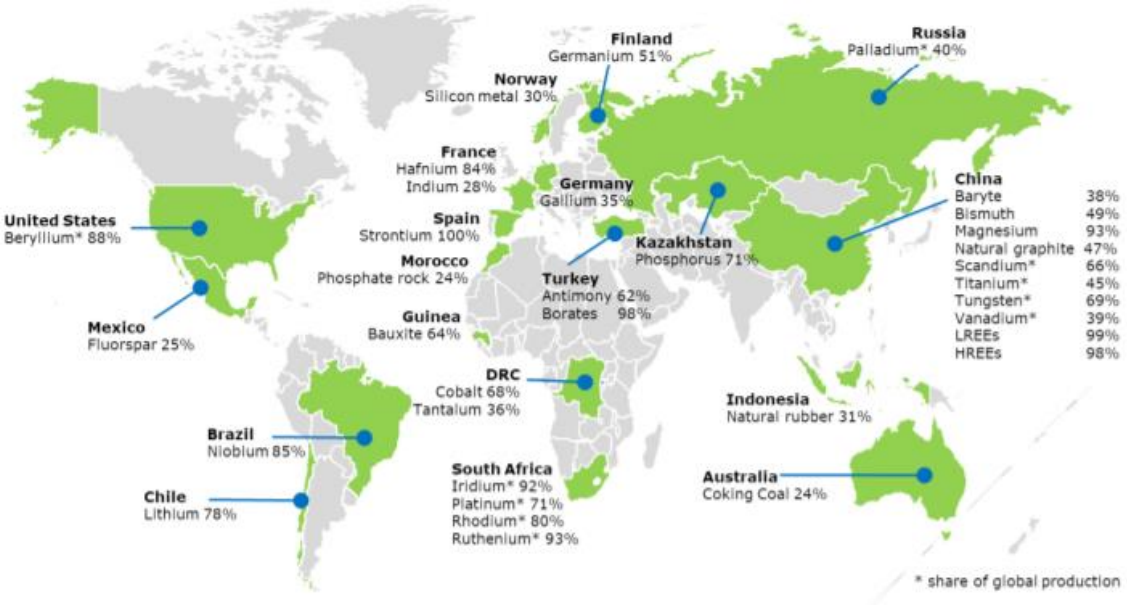

Figure 2.1. Biggest supplier countries of CRMs of EU (European Commission report on 2020 criticality assessment)

Currently, approximately half of the total greenhouse gas (GHG) emissions and more than 90% of biodiversity loss and water stress result from the extraction and processing of raw materials. Since only 12% of the materials used in the European economy come from recycling, there is a priority on increasing recovery and recycling rates (Smol *et al.*, 2020). Although several CRMs have a high technical and real economic recycling potential, and even with the

government incentives to adopt a circular economy, the recycling input rate of CRMs is generally low due to many factors: sorting and recycling technologies for many CRMs are not yet available at competitive costs; the supply of many CRMs is currently locked up in long-life assets, which implies delays between manufacturing and scrapping and has a negative influence on current recycling input rates; demand for many CRMs is growing in several sectors more than the recycling can meet that demand (EC, 2018).

A few CRMs, namely vanadium (V), W, Co and antimony (Sb), have a high recycling input rate. Other CRMs have a good recycling rate at end-of-life (e.g. recycling rates for platinum group metals (PGMs) reach up to 95% for industrial catalysts and 50-60% for automotive catalysts), however, this contribution is largely insufficient to meet the growing demand, for which the recycling input rate decreases (e.g. 14% for PGMs) (EC, 2018).

As it can be observed in Tables 2.1 and 2.2, most of critical raw materials are metals. The growing demand for metals and the depletion of high-grade primary ore reserves mean that residues from historic mining explorations can have higher metal grades than primary ores currently being excavated. The cost of extracting residual metals from mine tailings, which have already been part-processed, can be more economically attractive than mining a deep-buried primary ore body. Mine wastes may even contain metals (such as rare earth elements), which extraction was not considered valuable when the ores were initially processed but have recently increased in value and use. A representative case study was the cobalt-rich tailings from a former copper mine in Uganda, which were reprocessed by bioleaching decades after the local mining ended, both to extract Co and to remove the environmental risk (Falagán *et al.*, 2017).

However, metals can be functionally or non-functionally recycled. Through the previous one, the metal embedded in end-of-life products is separated, sorted, and sent back to raw material production processes, to be used again in the production of high-end products. In another case, the metal is collected and incorporated in a large-magnitude material stream, ending up in low-end products (downcycling) or as a contaminant. Although the metal is usually infeasible to recover in a large-magnitude stream, it can be dissipated in the technosphere instead of into the environment. Metals recycling depends on several factors such as the collection rate, pre-treatment efficiency, recycling processes efficiency, and type of available end-of-life products. If metal is present in certain products in very low concentrations (e.g printed circuit boards) or its use is intentionally dissipative (e.g. metals in medicines or pesticides), the metal recovery is not considered (Godoy León *et al.*, 2020).

In terms of recycling, certain limitations are imposed by how a particular material has been used: e.g. zinc is difficult to recycle once it has been dispersed across a large area, metallic surfaces, where it is typically applied in relatively low concentrations for galvanizing purposes. Since the recycling rate of different metals increases in proportion to their price,

improving scarcity (and price) can encourage more efforts to achieve higher recycling rates. However, (almost) full recycling is only likely to be approached when metals and other elements have become relatively expensive (Rhodes, 2019), so the mitigation of supply risk by substituting a CRM with a non-critical raw material with similar performance can also be considered in order to relieve CRMs dependency (EC, 2020b).

There is a growing concern about a potential shortage of critical elements and raw materials essential for modern technology, including those for low-carbon energy production. Even with a large increase in recycling rates for many materials, the full-scale deployment of a global renewable energy system will likely require replacing many of the scarcer elements for more Earth-abundant alternative materials. Ecodesign can provide creative solutions to reduce the use of CRMs across a wide range of products, adopting more robust and durable features (Rhodes, 2019), as well as innovative technological solutions for mining and processing CRMs based on automation and digitalization. For example, the remote sensing of Europe's earth-observation Copernicus Programme can be used to identify new CRMs sites and monitor the environmental performance of mines, neither during their operating life, but also after closure (EC, 2020b).

These sensing or digital technologies also allow the measurement of the operational and environmental parameters to ensure safety and efficiency, for example, with real-time monitoring of chemical processes parameters such as gases concentration, temperature, pressure, pH, and energy consumption. These so-called green chemistry principles (GCP) support the transition from a linear to a circular economy through the efficient use of natural resources and energy towards sustainable development (Chen *et al.*, 2020).

In addition to the technical aspects already mentioned and even considering the widely recognized potential of circular economy in a greater circularity of resources to contribute to sustainable development, the sustainable use of resources and improving human health must be increased to assess the European Green Deal. The practical implementation and quantitative evidence of beneficial effects of circular economy practices on the triple bottom line (economic, environmental, and social domains) need to be further explored (Velenturf *et al.*, 2019; Smol *et al.*, 2020).

2.1.1. Tungsten

General properties

Tungsten, also known as wolfram (chemical symbol W), is a hard and rare transition metallic element of group VI of the periodic table, with a greyish-white lustrous appearance. Tungsten is found in nature almost exclusively in primary minerals like scheelite ($CaWO_4$), wolframite ($[Fe/Mn]WO_4$), hübnerite ($MnWO_4$) or ferberite ($FeWO_4$), containing about 0.1-5%

WO_3 (Lassner & Schubert, 1999; Schwertberger, 2016). Tungsten is a CRM with a wide range of uses, being the largest in cemented carbides production, followed by mill products, alloys and steels (Cuesta-Lopez, 2017).

Tungsten is characterized by the second highest melting point (3420 °C) of any element, exceeded only by carbon (3550 °C). It has the lowest vapor pressure of all metals, the lowest compressibility, an extremely high density (19.3 g/cm^3), a high elasticity modulus, low thermal expansion, and high thermal conductivity. Pure tungsten has a body-centered-cubic structure, frail at room temperature, but acquires a ductile state at elevated temperatures (100-500 °C) (Lunk & Hartl, 2019; Midwest Tungsten Service, 2021). Tungsten has very peculiar characteristics, which are resumed in Table 2.3.

Generally, W deposits are formed by magmatic-hydrothermal processes combined with granitic intrusions. These deposits can be found inboard the periphery of the intrusive itself (greisen, porphyry, stockwork, and vein deposits) and in its surroundings (stockwork, vein and skarn deposits). Tungsten deposits are often related to molybdenum or tin mineralization (Schmidt *et al.*, 2012).

However, the primary tungsten-bearing ores commercially mined, scheelite and wolframite, are becoming gradually limited (Yang *et al.*, 2016). Additionally, due to the waste rock that needs to be removed to access the ore, W mines produce volume-wise more waste than has originally been mined. The accumulation of residues in open pits generates serious landscape and other environmental problems (Schmidt *et al.*, 2012).

Because of the mentioned reasons, the EU and the USA recognized W, respectively, as one of the 30 CRMs (European Commission, 2020), and as one of the 35 mineral commodities (U.S. Geological Survey, 2018) considered critical.

Chemistry

Tungsten has complex speciation with several oxidation states, from -2 to +6, which is the most common state. Tungsten normally occurs as the oxyanion tungstate WO_4^{2-} in the environment, which can polymerize with itself and with other ions, resulting in the formation of many classes of W complexes (Lunk & Hartl, 2019; Schwertberger, 2016). The interaction of W with aqueous solutions is quite complex, leading to a cascade of chemical reactions, which are difficult to control and identify. However, the weak corrosion resistance of W can be an advantage as an anode in an electrochemical cell to suppress the release of hydrogen (Nave & Kornev, 2016).

Table 2.3. General properties of tungsten (W) (*adapted from* Midwest Tungsten Service, 2021; Lassner & Schubert, 1999)

Atomic Number	74	Atomic Mass	183.86 u
Electron Distribution	$[Xe]4f^{14}\ 5d^4\ 6s^2$	Oxidation Number	-2, -1, 0, +1, +2, +3, +4, +5, +6
Melting Point	3420 °C	Boiling Point	5530 °C
Electronegativity	2.36	Isotope	180, 182, 183, 184, 186
Density	19.3 g/cm³	Atomic Volume	9.53 cm³/mol
Ionization Energy	770 kJ/mol		

Tungsten can be considered an inert metal that is resistant to many elements and compounds such as molten metals, being stable to mineral acids in the cold and only slightly attacked at higher temperatures. Table 2.4 shows the reactivity of W in aqueous solutions of mineral acids and alkalis, demonstrating that majority do not attack W. However, the presence of oxidizing agents in combination with acids or alkalis can result in rapid dissolution (Lassner & Schubert, 1999).

Table 2.4. Reaction of tungsten metal with acids and alkalis (Lassner & Schubert, 1999)

Reagent	**Temperature**	
	20 °C	100-110 °C
HF	None	None
HNO_3	Slight attack	Oxidation
H_2SO_4	None	Slight attack
HCl	None	Slight attack
H_3PO_4	None	Slight attack
H_2O_2	None	Dissolution
NH_4OH	None	None
KOH	None	None
NaOH	None	None
HCl + HNO_3	Oxidation	Dissolution
HF + HNO_3	Dissolution	Dissolution
KOH + H_2O_2	Slight attack	Dissolution

Table 2.4 also alludes to important acid mixtures to dissolve tungsten. 40% HNO_3 and 60% hydrofluoric acid (HF) could be a good mixture because W is strongly attacked at room temperature. HF is a weak acid, so does not ionize completely. The metal surface is oxidized by NO_2, and the tungsten oxide dissolves in HF, generating tungsten fluoride (WF_6) or oxofluoride ions with high solubility. Here, there is no complexing agent like fluoride as in the former acid mixture, so an oxide layer is formed which slows down the reaction. W

dissolution by HNO_3:HCl mixture (aqua regia) is slowly at room temperatures (~20 °C) but rapid in hot (100-110 °C) (Lassner & Schubert, 1999).

Nonetheless, HF is an unpleasant acid (extremely corrosive, produces severe burns, and attacks bones hours after exposure) and very reactive acid. Thus, it should only be used by experienced chemists familiar with its properties and who know what precautions to take.

The electrochemical behavior of W in aqueous solutions is very closely related to two facts: the high affinity of W to oxygen, which always leads to the formation of an irreversible metal/metal oxide/metal ion system, and the complexity of W species in aqueous solution. Despite this, tungsten species in aqueous solutions can react with a variety of chelating agents with polycarboxylic acids like oxalic, tartaric, or citric acid, which can be used to stabilize acidic tungsten solutions (to prevent polycondensation) (Lassner & Schubert, 1999).

The interpretation of the said complex tungsten oxides at low voltages can bring new technological developments in electrical tungsten recovery. In this way, Figure 2.2 represents possible thermodynamically stable phases of W species (at chemical equilibrium) of an aqueous electrochemical system (Nave & Kornev, 2016). This graphic representation of electrochemical potential (i.e. energy required for oxidation) *vs* pH is called a Pourbaix diagram. It is basically a demonstration of the potential at which electrochemical redox reactions occur at the surface of an electrode in an aqueous electrolyte, and the element electrochemical properties are pH-dependent (Schweitzer & Pesterfield, 2010; Jun *et al.*, 2019).

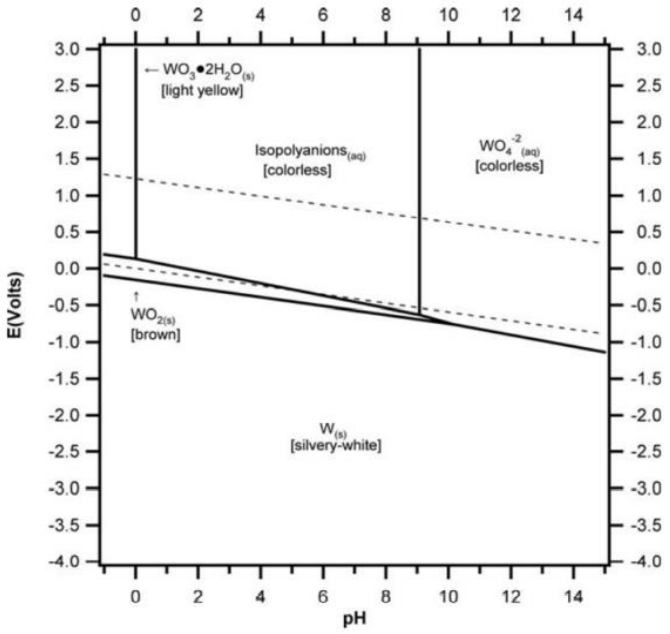

Figure 2.2. E-pH diagram for W species. Soluble species concentrations (except H^+) = $10^{-1.0}$ M. Soluble species and most solids are hydrated. No agents producing complexes or insoluble compounds are present other than HOH and OH^- (Schweitzer & Pesterfield, 2010).

Tungsten has good corrosion resistance properties, but metallic W is not thermodynamically stable in water at 25 °C (Jun *et al.*, 2019). Electrodeposition of W is only possible when the hydrogen formation is blocked, which is influenced by thermodynamic and kinetic properties. Due to several oxidation states, W solutions can form both cathode and anode reactions. Therefore, it is only possible to deposit W from aqueous solutions together with alloying elements such as Co, Fe, Ni, or Cu (Lassner & Schubert, 1999). There are several identified reactions in aqueous solutions:

$$WO_2\,(s) + 4H^+(ads) + 4e^- \rightarrow W(s) + 2H_2O$$

$$W_2O_5(aq) + 2H^+(ads) + 2e^- \rightarrow 2WO_2\,(aq) + H_2O$$

$$2WO_3(s) + 2H^+(ads) + 2e^- \rightarrow W_2O_5(aq) + H_2O$$

$$WO_4^{2-}(aq) + 2H^+(ads) \rightarrow WO_3(aq) + 2H_2O$$

$$WO_4^{2-}(aq) + 8H^+\,(ads) + 6e^- \rightarrow W(s) + 4H_2O$$

$$WO_4^{2-}\,(aq) + 4H^+(aq) + 2e^- \rightarrow WO_2(aq) + 2H_2O$$

$$2WO_4^{2-}\,(aq) + 6H^+(aq) + 2e^- \rightarrow W_2O_5(aq) + H_2O$$

WO_2 and WO_3 are the most thermodynamically stable oxides. As indicated by the Pourbaix diagram (Figure 2.2), as the pH drops to neutral and acidic conditions, different polytungstate ions (also called isopolyanions) are formed. These ions can react with water to form a light pale-yellow $WO_3.2H_2O$ (s) which precipitates when the acidity becomes high (Schweitzer & Pesterfield, 2010; Nave & Kornev, 2016).

In aqueous alkaline solutions, tungsten forms tungstate ions WO_4^{2-}(aq). Metallic W as an anode in basic solutions is dissolved electrolytically (oxidized to the hexavalent state) (Nave & Kornev, 2016; Lassner & Schubert, 1999):

$$W\,(s) + 8OH^-(aq) \rightarrow WO_4^{2-}(aq) + 6e^- + 4H_2O$$

Production

Figure 2.3a indicates the global average distribution of W mining production between 2012-2016. China is largely the major producer of primary W, accounting for 82% of global production (i.e. 73 000 t), followed by Vietnam as the second-largest producer (i.e. 5 600 t (2015), accounting for only 4% of the world market (EC, 2020a; Tkaczyk *et al.*, 2018).

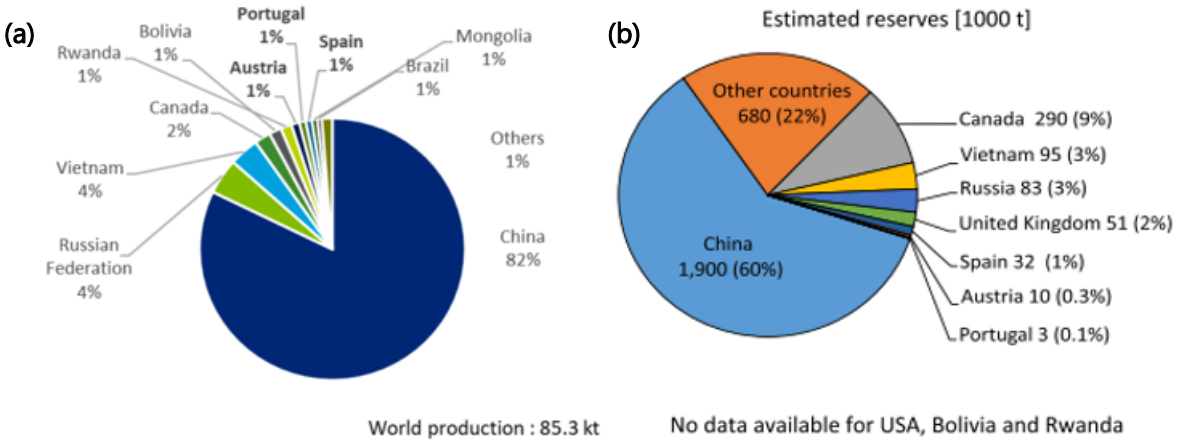

Figure 2.3. a) Global share of W mining production for 2012-2016 (EC, 2020a); and b) estimated W reserves based on USGS data (Tkaczyk *et al.*, 2018).

Regarding the estimated W reserves (Figure 2.3b), China also largely ranks first place, possessing ~60% of the world's W deposits. The next largest W reserves are in Canada (9%), Russia and Vietnam with (3%), the United Kingdom (2%), Spain (1%), Austria (0.3%), Portugal (0.1%), and then 22% in other countries. Some countries of global distribution shares show little variations among surveys (Shemi *et al.* (2018) or EC (2020a) data) because USA, Bolivia and Rwanda are not included (Tkaczyk *et al.*, 2018).

Tungsten mining is predominantly an underground operation, while open-pit mining is restricted to exceptional cases. The mines are typically not very large and are limited by the size of the ore bodies. Rarely, more than 2000 tons of ore *per* day is produced, although recently there are mines with rates of up to about 5 500 tons of ore *per* day. Internationally traded ore concentrates require 65–75% WO_3, which means the need to mine a huge tonnage of ore just to obtain a small amount of W. To reach the international requirements mentioned, the very huge amount of gangue material must be separated, and it is usually deposited as tailings. Therefore, ore processing plants are always located close to the mine to save on transportation costs (Shemi *et al.*, 2018).

The global demand for W increased from 62 550 tons in 2005 to 82 500 tons in 2015. In 2015, China was the highest consumer of W (64%) followed by Europe (14%), USA (9%), Japan (7%), and others (6%) (Cuesta-Lopez, 2017).

The increase of the world demand for W has been closely tied to general economic activity, especially due to China's GDP increase. However, the W consumption in Europe has been decreasing about 5% on average since 2002, because W products are mostly used in mature industrial applications rather than in some novel and evolving technologies. Thus, the decrease of W consumption could be attributed to the lower economic growth rates in Europe,

but since 2013 a demand for W in Europe seems to slightly increase, with a tendency to continue (Hartmann *et al.*, 2016).

Even though the consumption of W continues to increase as the amount of carbide tool production increases with the expansion of markets in developing countries (EC, 2020a), the tungsten produced in Europe, including the mine production and the production from the end-of-life scraps recycling, could meet 80% of the demand (Hartmann *et al.*, 2016). If Europe could take full advantage of its resources, primary and secondary, the dependency on other countries to produce hard metal tools could be overcome (Almeida *et al.*, 2021).

Applications

Figure 2.4 shows a schematic of the global mass flow of tungsten through its entire supply chain in 2010, as well as the energy requirements of key transformation processes and the material grades of main flows (Leal-Ayala *et al.*, 2015).

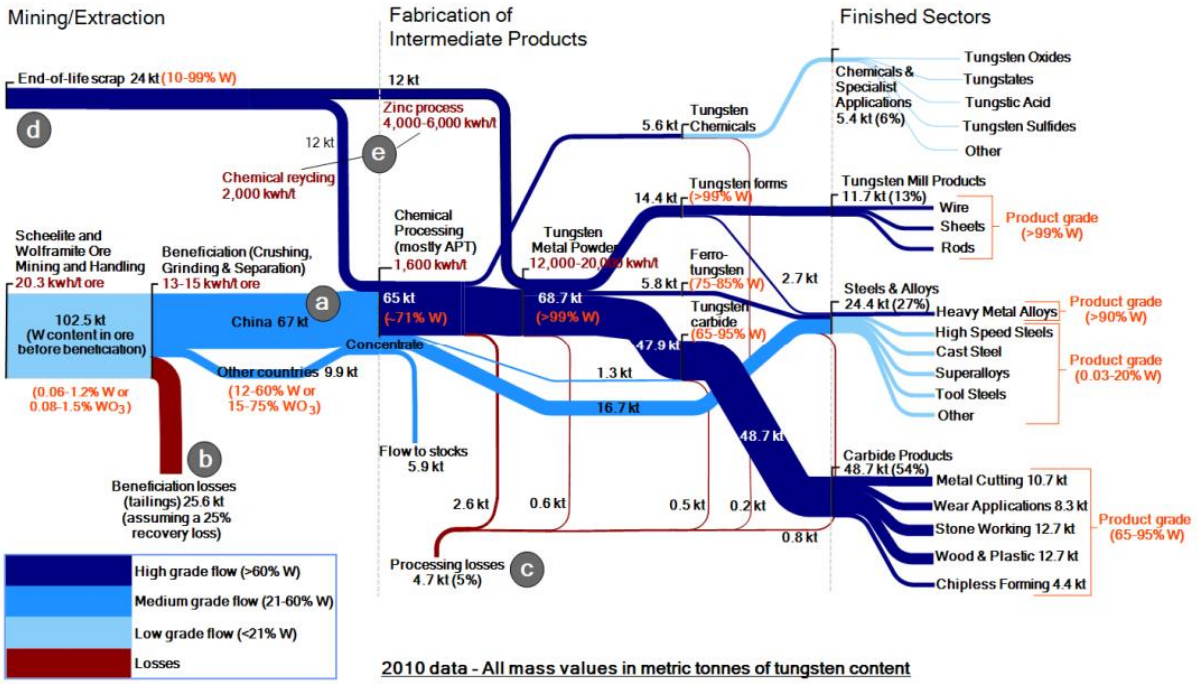

Figure 2.4. Global mass flow for tungsten in 2010. The grade of different flows and the energy consumption of selected processes are indicated with orange and red text respectively (Leal-Ayala *et al.*, 2015).

The exceptional properties of W make this metal essential for technological applications under extreme conditions. Tungsten has various industrial applications, and recent data from the British Geological Survey and USGS (2017), represented in Figure 2.5, shows new four main branches to classify modern applications of W. Cemented carbide tools manufacture is still the most widespread use of W, with around ~54% of global average W consumption. Tungsten applications have evolved to the production of catalysts, electrical and electronic

components, including, for example, photocatalysis based on W-containing-nanomaterials and electrocatalytic applications for fuel cells (Tkaczyk *et al.*, 2018).

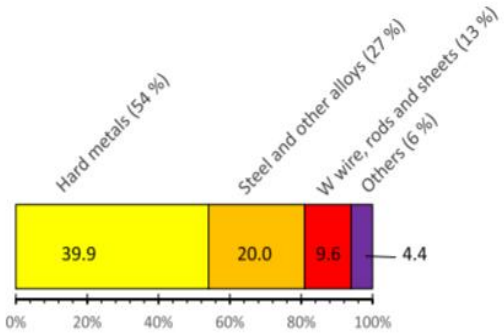

Figure 2.5. Main application areas of W, including annual production in 1000 (t) (respective share is in percentage (Tkaczyk *et al.*, 2018)).

2.1.2. Cobalt

General properties

Cobalt (chemical symbol Co) is a silvery-gray transition metal characterized by important properties, such as hardness, wear-resistance when bonded with other metals, low thermal and electrical conductivity, high melting point (1493 °C), high thermostability and multivalences, with different applications from industry to medicine. Cobalt is also known to produce intense blue colors when combined with silica and to retain ferromagnetic properties at the highest temperature of any metal (Slack *et al.*, 2017; Yildiz, 2017).

Cobalt is not found pure in nature, but rather in multiple and widespread minerals and compounds containing it, although the important deposits may differ in geologic, geochemical, mineralogic, and other terms. The main deposit types are stratiform sediment-hosted Cu-Co deposits, Ni-Co laterite deposits, and magmatic Ni-Cu(-Co-PGE) sulfide deposits (Slack *et al.*, 2017).

Cobalt is one of the abundant metals on Earth, with global reserves of around 7 million tons (Yildiz, 2017). Although this element plays an essential role in the performance of the products where it is used, there have been some efforts to preserve it, because of periods of high prices and the crescent concern about availability. However, in many applications, the replacement of Co would represent a loss in product performance and/or increased cost (Slack *et al.*, 2017).

Chemistry

Cobalt has some inorganic compounds and complexes, whose principal chemical and physical properties are mentioned in Table 2.5. Cobalt generally forms cobalt (II) and cobalt (III) compounds, but there are also rare Co compounds with +4, +1, 0, -1 oxidation states (Yildiz, 2017).

Table 2.5. General properties of cobalt (Co) (Yildiz, 2017)

Atomic Number	27	Atomic Mass	58.93 u
Electron Distribution	[Ar]$3d^7$ $4s^2$	Oxidation Number	+2, +3
Melting Point	1495 °C	Boiling Point	2870 °C
Electronegativity	1.8	Isotope	59
Density	8.9 g/cm^3	Atomic Volume	6.7 cm^3/mol
Ionization Energy	757.6 kJ/mol		

Generally, Co (II) compounds dissolve in water. Cobalt gives cobalt (II) chloride by dissolving in dilute hydrochloric acid (HCl), exhibiting pink shades. This dissolution is slowly, instead of nitric acid (HNO_3) which dissolves faster and produces the Co^{2+} ions (Yildiz, 2017).

$$\textit{Dilute HCl: } Co + 2HCl \rightarrow CoCl_2 + H_2$$

$$\textit{Dilute } HNO_3\textit{: } 3Co + 8HNO_3 \rightarrow 3Co(NO_3)_2 + 2NO + 4H_2O$$

Another oxidation number of Co is +3, however, this ion can only be found in the complex, being the Co (III) ions less stable than the other compounds. Pure Co releases oxygen from acidic and neutral environments. All Co oxides dissolve in HCl. Examples of common Co compounds are Co salts such as cobalt (II) sulfate, cobalt nitrate, and cobalt (III) sulphate (Yildiz, 2017).

Figure 2.6 represents the Pourbaix Diagram for Co, with possible thermodynamically stable phases of Co species (at chemical equilibrium) of an aqueous electrochemical system (Garcia *et al.*, 2008).

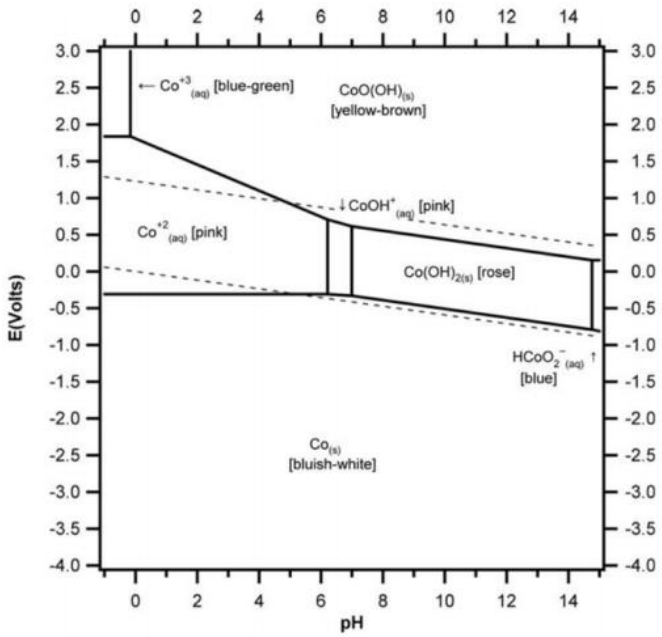

Figure 2.6. E-pH diagram for Co species. Soluble species concentrations (except H^+) = $10^{-1.0}$ M. Soluble species and most solids are hydrated. No agents producing complexes or insoluble compounds are present other than HOH and OH^- (Schweitzer & Pesterfield (2010))

Electrodeposition in aqueous solutions is an important process in the production of metallic Co. It has been reported that Co electrodeposition at pH < 4 occurs together with a hydrogen detachment reaction. During this electrodeposition, a hydrogen-rich phase can be adsorbed, as represented by the following equations (Garcia *et al.*, 2008):

$$Co^{2+}(aq) + 2e^- \rightarrow Co(s)$$

$$H^+(aq) + Co(s) + e^- \rightarrow CoH(ads)$$

$$H^+(aq) + CoH(ads) + e^- \rightarrow Co(s) + H_2(ads)$$

$$\textit{Total: } Co^{2+}(aq) + 2H^+(aq) + 4e^- \rightarrow Co(s) + H_2(ads)$$

In the cobalt electrodeposition process at pH > 4, Co deposits as Co hydroxide ($Co(OH)_2$) at the interface electrode solution (chemical stage). This interface electrode solution becomes alkaline due to the water electrolysis, inducing the precipitation of the $Co(OH)_2$ as shown in the Pourbaix diagram (Figure 2.6). Here, the Co electrodeposition occurs directly, although the process contains the formation of a Co hydroxide intermediate (Garcia *et al.*, 2008), which can be described by the following equations:

$$2H_2O + 2e^- \rightarrow 2OH^-(aq) + H_2(g)$$

$$Co^{2+}(aq) + 2OH^-(aq) \rightarrow Co(OH)_2(s)$$

$$Co(OH)_2(s) + 2e^- \rightarrow Co(s) + 2OH^-(aq)$$

$$\textit{Total: } Co^{2+}(aq) + 2H_2O + 4e^- \rightarrow Co(s) + 2OH^-(aq) + H_2(g)$$

Basically, Co is always covered by a native passive film which consists mainly of CoO or $CoO.H_2O$, which is unstable in acidic solutions. In neutral solutions, CoO tend to be stable, while in basic solutions the $Co(OH)_2$ passive film undergoes further oxidation to Co(III) compounds (CoOOH and/or Co_3O_4), depending on the electrode potential and the pH of the solution (Badawy *et al.*, 2000).

Production

Cobalt is generally mined as a byproduct of more abundant metals, such as nickel or copper, so the production is primarily driven by the markets for the principal metals, not by the need for Co. This situation limits the flexibility to adjust the amount of Co extracted in response to the demand fluctuations and can result in periods of shortage or oversupply (as occurred from 2009 to 2015 when global Co production exceeded the consumption, leading to a surplus market and negative pressure on prices) (Slack *et al.*, 2017).

Annual global Co consumption was approximately 75 000 metric tons in 2011; China, Japan, and the United States (in order of consumption amount) were the top three Co-consuming countries (Slack *et al.*, 2017). In 2016, approximately 126 000 metric tons of Co were mined produced in ores, concentrates, and intermediate products from cobalt, copper, nickel, platinum group element (PGE), and zinc operations (Alves Dias *et al.*, 2018).

Figure 2.7 reveals the distribution of Co deposits according to the world's Co mine production in 2011. Democratic Republic of Congo (Congo Kinshasa or DR Congo) is the principal source of mined Co in the world (55%). This country has a high-risk index for doing business because of poor infrastructures, resource nationalism, a high perception of corruption, and a lack of transparency, as well as wars during the 1990s to early 2000s, living in a persistent tension in the eastern part of the country with a substantial risk of civil war, which can mean instability in Co supply. Although civil unrest in the eastern part of DR Congo has not affected the Co-producing areas, problems with infrastructure (especially energy and transport) and reviews of and changes to mining contracts have slowed some of the potential growth in mine development and production. However, the copper-cobalt mining industry in DR Congo has significantly recovered from the collapse in production that occurred in the 1990s (Slack *et al.*, 2017).

China has been the leading refiner of Co, and much of its production came from primary materials imported from DR Congo. Other significant sources of refined Co were Australia, Belgium, Canada, DR Congo, Finland, Norway, and Zambia (Slack *et al.*, 2017). EU production was estimated at 2300 tons, all sourced from Finland (Alves Dias *et al.*, 2018).

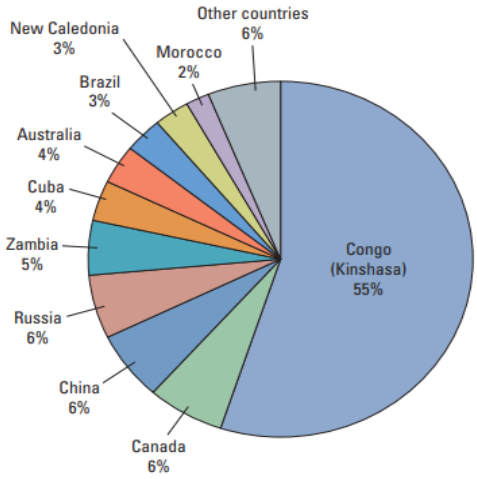

Figure 2.7. Pie chart of cobalt's mine distribution by countries (Slack *et al.*, 2017).

The USA has a great reliance on imports for its Co needs, only producing a negligible amount of byproduct Co as an intermediate product from a PGE mining and refining operation in Montana. Recently, between 75-80% of the USA cobalt supply has come from imports and releases from the National Defense Stockpile; the remaining 20-25% percent has been from recycled scrap. This high reliance on imports increases the potential for supply disruption and high prices during supply shortfalls (Slack *et al.*, 2017).

Because of the mentioned reasons, the EU and the USA recognized Co, respectively, as one of the 30 CRMs (European Commission, 2020), and as one of the 35 mineral commodities considered critical to U.S. National Security and Economy (U.S. Geological Survey, 2018). To avoid this problem, there have been several researchers pushing towards the identification of materials suitable for Co replacement or improving and turning the recycling processes more efficient. However, as the possible substitutes of Co are often combined with potential reductions in product performance, recycling should be very interesting, with several publications reporting Co recovery to efficiencies of 60%–100% from secondary resources, including recycling mining residues or end-of-life lithium-ion-batteries (Tkaczyk *et al.*, 2018).

Applications

Cobalt's diverse uses can be divided into two broad categories: chemical and metallurgical. Rechargeable batteries belong to the first group and have largely contributed to the rapid growth of Co demand, increasing from 28% of total Co consumption in 2010 to 49% in 2015 (Figure 2.8). Pigments, catalysts, dryers, and other minor chemical end-uses have less than 20%. The remaining end sectors, which belong to metallurgical uses, consist of superalloys, which represented 18% of total consumption in 2015, hard metals, magnet alloys, hardfacing alloys, high-speed steels, and special alloys (EC, 2020a; Alves Dias *et al.*, 2018).

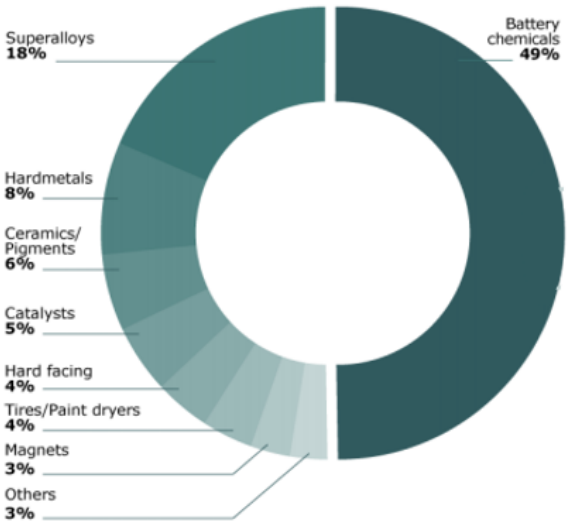

Figure 2.8. Refined cobalt demand by end-use in 2015 (*adapted from* Alves Dias *et al.*, 2018)

Superalloys provide high-temperature service in several critical applications such as jet engines, gas turbines, space vehicles, nuclear reactors, and power plants. Superalloys can be divided into three categories: Co, nickel, or iron-based alloys. Cobalt is used in superalloys as the matrix or as an alloying element because of its high melting point and greater corrosion resistance at high temperatures, being present in Co-based and nickel-based alloys, which represent 6% and 80%, respectively, of the superalloy production. Cobalt-based forged alloys contain around 30% of Co, and Co-based cast alloys can contain up to 65% of Co. Cobalt-based superalloys provide higher melting points than nickel (or iron) alloys, superior resistance to hot corrosion in gas turbine atmospheres, and excellent thermal fatigue resistance and weldability over nickel-based superalloys (EC, 2020a).

Hardfacing alloys refer to the deposition of hard alloys by a welding process onto a softer metal to protect it from wear, such as Co, chromium, molybdenum, or nickel. Cobalt-based hardfacing alloys are selected for their excellent resistance to the widest combination of wear types, with the cobalt typically reaching 40% to 60% (EC, 2020a).

The called hard materials include cemented carbides and diamond tools. Cobalt powder is used as the binding material in the production of cemented carbides, mainly produced from W, to increase resistance to wear, hardness, and toughness, crucial qualities for cutting tools and wear-resistant components used by the metallurgy, mining, oil drilling, and construction industries (EC, 2020a).

In chemical applications, Co is used for a wide range of chemical compounds, with an emphasis on rechargeable batteries (EC, 2020a). This element is considered as a limiting factor in the development of lithium-ion batteries (LIBs) (Alves Dias *et al.*, 2018), which are used for the power supply of several electronic equipments. In LIBs, Co is present as lithium cobalt

oxide ($LiCoO_2$), in a concentration 5%–20% higher than in usual Co-containing minerals. The EC considers LIBs as an emerging technology, which leads Co demand to increase in the future, but also refers to the potential attractivity for recycling (EC, 2020a; Tkaczyk *et al.*, 2018).

Cobalt studies are continuing since they have a wide variety of functions and many applications, including agriculture, medicine, and pharmaceutical technology (Yildiz, 2017; Godoy-León & Dewulf, 2020).

2.1.3. Tungsten carbide

To understand the properties of tungsten carbide (WC), it is relevant to briefly summarize the reaction of W with carbon and carbon-containing compounds. The carburization of W powder is the most widely used process for producing WC (Lassner & Schubert, 1999).

Tungsten carbide can be defined as an interstitial carbide, due to its characteristics of both ceramics and metals. Although there are several methods for WC powder synthesis, almost all of them are based on direct carburization of W (average particle size: between 0.15 to 12 μm) or carbothermal reduction of W oxide to pure W and consequent carburization. Hexagonal WC is the dominant phase of WC, with a density of 15.63 g/cm^3, a melting point of 2870 °C, and a boiling point of 6000 °C. WC can be decomposed in W and C at high temperatures, and its oxidation starts at 500–600 °C (Lunk & Hartl, 2019; Yang *et al.*, 2016).

Generally, the usual carburization temperatures for W powder and black C mixtures range between 1050 °C and 2100 °C, depending on the powder particle size. This wide temperature range can be explained by the influence of the properties of the starting materials (W and C) as well as several other parameters, with the most common temperature range being 1400–1600 °C. Furthermore, the purity of W influences carburization. Metals like Co are an example of a combination that accelerates carburization, while alkaline metals retard it (Lassner & Schubert, 1999; Lunk & Hartl, 2019).

Tungsten carbide is extremely hard, rated around 9 on the Mohs hardness scale. Cemented carbide, which represents by far the largest consumption of W worldwide, consists of fine particles of carbide cemented into a composite by a binder metal. The hard material phases of WC are bonded together by a ductile metallic phase that surrounds them (often Co, more rarely Ni or Fe alloys) (Lunk & Hartl, 2019).

The most common cemented carbide is tungsten carbide-cobalt (WC-Co), a composite material consisting of tungsten monocarbide particles embedded within a Co binder providing an optimal solution as tools and components for metal cutting, rock drilling, and wear resistance applications. They are widely used in the manufacturing, mining, construction, oil, and gas sectors. This composite typically contains between 40–95% W, being the most metallic of the carbides (Seo & Kim, 2016; Shemi *et al.*, 2018).

The Co content and WC grain size determine the mechanical properties of WC-Co, which can be adjusted to obtain desirable properties for specific applications (Lassner & Schubert, 1999). Improving the Co content results in less hardness and higher toughness, while a larger grain size increases the toughness and decreases the hardness (Furberg *et al.*, 2019).

Production

Although the global tungsten mine production is indeed dominated by China at about 80%, less than half of the global production of cemented carbides occurs in China and only 23% of that was exported in 2015 (Furberg *et al.*, 2019).

WC production occurs normally by two steps: the step of producing high purity W powder with desired properties and the step of W powder carbonization by high purity black carbon black, soot, or graphite. The carbonization step is implemented by (i) mixing the W powder with carbon black, soot, or graphite by ball milling and (ii) carbonizing W powder at temperatures of 1400-1600 °C in a hydrogen atmosphere for 2-10 hours (Yang *et al.*, 2016).

Several innovative W powder production processes have been emerging. The future trend for WC production points towards the direct reduction of tungsten oxide (WO_3) or tungsten ore concentrate, reducing the current heavy and expensive two-step production process (tungsten powder production + carbonization) into a single-one step. This new process has another advantage of producing WC powder with a finer nanometer crystal structure and improved mechanical properties (Yang *et al.*, 2016).

Applications

Figure 2.9 shows the distribution of applications of WC materials in various industries due to their incredible wear resistance and excellent corrosion resistance properties. While WC cemented with Cu or Ag is used for making the electrical contacts and in fuel cells, tungsten carbide with cobalt (WC-Co) is preferred for cutting tools due to its very high abrasion resistance, compressive strength and withstand higher temperatures than standard high-speed steel tools, with a sharp cutting edge and a better surface finish. WC is also used

for so distinct things from the ball in the tips of ballpoint pens to projectiles and anti-missile warheads (Katiyar & Randhawa, 2020).

The Co content in WC-Co hard metal machining tools is frequently between 6 and 16 wt%, although it reaches 30 wt% for rare applications. In the case of 6% Co, it corresponds to tools requiring high hardness, used for metal cutting, mining, and wood working, and in the case of 16% cobalt to higher toughness tools, required for cold forming and hot rolling (Furberg *et al.*, 2019). After industrial use, these scraps must not be buried underground to avoid groundwater contamination with dissolved Co, which is also dangerous to the human respiratory system (Lunk & Hartl, 2019; Seo & Kim, 2016).

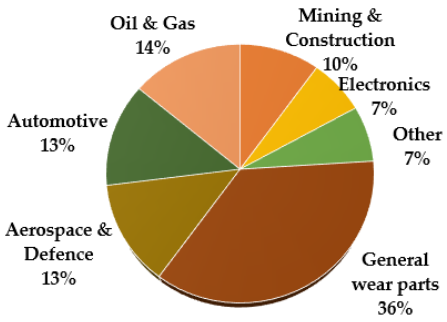

Figure 2.9. Distribution of WC applications for different sectors (Katiyar & Randhawa, 2020).

2.1.3.1. Tungsten carbide recovery

The recycling activities inside Europe have considerably increased since the global economic crisis in 2009. Experts reported a recycling rate for W in the EU as high as 45-50%. The recycling input rate from new and old scrap for W was estimated at 35% and the estimated end-of-life recycling rate was up to 30% (EC, 2020a). However, the excellent physical and chemical stability of W makes the recycling process extremely challenging (Xi *et al.*, 2017).

The recycling of WC-Co hard metal scraps can avoid its harmful effects on the environment, and there are many techniques to perform recycling processes (Seo & Kim, 2016). Depending on the type of cemented carbide conversion method applied, Shemi *et al.* (2018) the recycling processes can be classified into three categories:

- Direct methods, which transform the supplied material to powder of the same composition;
- Indirect methods, which involve chemical modification of the component metals into intermediate products that are then processed to obtain pure metals;

- Semi-direct methods, which chemically dissolve one component leaving the other phase(s) intact.

In the direct method, the binding metal is separated from the cemented carbide preserving the same composition, while in the indirect method, the binding metal is dissolved. Direct recycling techniques, such as zinc or cold flow processes, are characterized by low energy consumption, low process costs, and a high recycling rate of carbide scrap recycling rate. Instead, indirect recycling processes use acids and electrochemistry to dissolve the binder phase in cemented carbide waste. In this method, there is high energy consumption, high process costs, and a low recycling rate of the carbide scrap (Rizzo *et al.*, 2020).

The recycling of tungsten-bearing waste has been established for several decades (see Wainer, 1956), involving much R&D work focused on improving the previous methods as well as developing new ones. However, it is still necessary to seek more process innovation on issues such as energy efficiency, cost savings, resource preservation, and environmental regulation (Shemi *et al.*, 2018).

The conventional recycling methods typically recover WC-Co waste as a mixed powder of WC particles and Co binder, but some methods try to recover W or Co selectively. WC-Co particles can be processed through hydrometallurgical steps, with the W dissolution or leaching efficiency being increased by prior oxidation of WC-Co waste (Seo & Kim, 2016). Conventional recycling also uses alkaline solutions, so while W is obtained as $CaWO_4$, Co contained in the raw material is not recovered because Co is precipitated in alkaline solution. Thus, a broad need arose to establish the environmentally friendly recovery process of W and Co simultaneously with unheated oxidation, room temperature, and pressure leaching (Shibata *et al.*, 2012).

The purpose of the normal processes is the dissolution (selective anodic leaching) of binder (Co) or W or even both. Mainly, the recycling process comprises a selective breaking or electrochemical removal of the binder phase (matrix phase) or WC (dispersed phase) with the presence of acidic and/or alkaline electrolytes (Katiyar & Randhawa, 2020).

Acid leach milling or wet milling was suggested to dissolve W or Co from soft scraps of WC-Co in strong inorganic acids to increase the dissolution rate (Seo & Kim, 2016). However, strong inorganic acids (such as hydrochloric acid (HCl), phosphoric acid (H_2SO_4), and nitric acid (HNO_3)), widely used due to their high efficiency) are dangerous to the environment because they emit toxic gases as Cl_2, SO_3, and NOx during leaching (Sun *et al.*, 2017).

Anyway, selective Co extraction with organic acids was very rare because the Co dissolution rate in an organic acid is slower than in strong inorganic acids. For that reason, Co is selectively dissolved from WC-Co waste using mainly strong inorganic acids. More recently, researchers discovered that some organic acids such as citric acid, oxalic acid, and

malic acid showed high efficiency to dissolve divalent metals from Co concentration when compared with several organic acids under the same dissolution conditions (Seo & Kim, 2016). Malic acid and citric acid, for example, have led an efficient Co leaching from an active oxide material ($LiCoO_2$) in spent LIBs, with more than 90% Co obtained under optimal conditions (Li *et al.*, 2010). The use of these acids can be eco-friendly, not only as a reagent in leaching operations but also as part of other recycling processes to recover CRMs, such as Co and Li.

Besides the established and industrialized recycling processes of WC materials based on the pyro, hydro, and combination of both, there are some WC recycling techniques under development supported by a considerable amount of R&D work in the improvement of W waste processing (Katiyar & Randhawa, 2020). The focus of this work is precisely on one of these methods under development, the electrochemically based techniques. The principal recycling methods of WC waste will be summarized next.

I. Zinc process

The zinc recycling process is the most widely used direct recycling process of the cemented carbide at an industrial scale (Shemi *et al.*, 2018).

The WC scrap heating (~900-950 °C) is assisted by the introduction of argon gas and is then distilled by vacuum. In this process, the selective dissolution of Co takes place at high temperatures (800 °C) in a molten Zn bath, followed by Zn evaporating (distillation process) around 950 °C under an inert atmosphere. Cobalt precipitation occurs due to the high melting point (1495 °C as compared to Zn at ~950 °C). After the selective dissolution of Co from the matrix, a finely divided WC material is obtained. There is a great energy consumption, about 4000 to 6000 kWh is requested for only one ton of WC (Lin *et al.*, 1995; Katiyar & Randhawa, 2020).

II. Cold stream process

Similar to the zinc process, the cold stream process requires inevitably a lot of energy and costly specialized equipment. The cold stream flow method includes heating cemented carbide scrap to a high temperature, injecting a high-speed cold air flow to the scrap to break and separate the scrap, and then recovering WC (Shemi *et al.*, 2018; Lin *et al.*, 1995).

III. Chlorination process

In this recycling process, the WC-Co scrap is initially chlorinated (exposed to a chlorine atmosphere at high temperature) to form metal chlorides. Following, they can be submitted to two steps: mechanical reduction for producing WC powder; or acidic/alkaline leaching to obtain intermediate byproducts such ammonium paratungstate, ammonium tungstate, or tungstic acid (Katiyar & Randhawa, 2020).

IV. High-temperature oxidation process

It is a high-temperature process operated at the above melting point of the binder phase that causes the swelling in scrap materials. The porous mass of WC is obtained and followed by subsequent mechanical reduction operation to get the very fine powder of WC. However, this process also requires a huge energy consumption (Katiyar & Randhawa, 2020).

V. Hydrometallurgical process

Hydrometallurgical recycling consists of immersing WC materials into the leaching solution to dissolve the binder material and leave the WC residue. This is further processed by grinding operations and reused for WC components manufacturing. However, the hydrometallurgical-based recycling process is mainly for the grinding sludge, W-Cu, soft scraps, and solid scraps that can be treated by various acidic/alkaline media. Binder materials are usually leached out from the WC materials. The leaching process can be accelerated in the strong acid/oxidizing environment (aqua-regia/H_2O_2) after optimizing the several leaching parameters (temperature, pressure, and pH of the solution, stirring speed, and strength of the leaching solution). Recycling on a hydrometallurgical basis is generally more expensive than the direct recycling process due to significant separation and the purification steps required to get a pure form of the product. However, selective Co leaching can reduce the number of steps and increase the energy efficiency of the process (Katiyar & Randhawa, 2020).

Figure 2.10 resumes a good example of a hydrometallurgical recycling process of W and Co from WC tool waste proposed by Shibata *et al.* (2012), which uses solvent extraction and crystallization-stripping methods. This method has two distinct parts: the acid leaching and the mechano-chemical (MC) treatment of WC residue.

W and Co were separated in the leaching step using diluted H_2SO_4 to Co dissolution. Cobalt ions in the leachate are extracted with di-2-ethylhexyl phosphoric acid (D2EHPA) by a cation-exchange reaction. The WC in the residue after H_2SO_4 leaching must be oxidized to dissolve in an aqueous solution. The MC treatment is suitable for oxidizing WC in the presence of $KMnO_4$ as an oxidation agent, and then K_2WO_4 is formed to dissolve in an aqueous solution without heating. Tungsten species remaining in the leachate can be extracted by tri-octyl amine as an anion-exchange reaction (Shibata *et al.*, 2012).

Oxalic acid leads the crystallization-stripping of Co, while W organic phase is treated by the crystallization-stripping with NH_4OH-NH_4Cl solution. The rare metals in the organic phase are recovered as insoluble salts such as cobalt oxalate (CoC_2O_4) and ammonium salts like ammonium paratungstate. Both crystallization products are transformed to metal oxides

by heating above 300-500 °C, much lower temperatures than conventional processes (Shibata *et al.*, 2012).

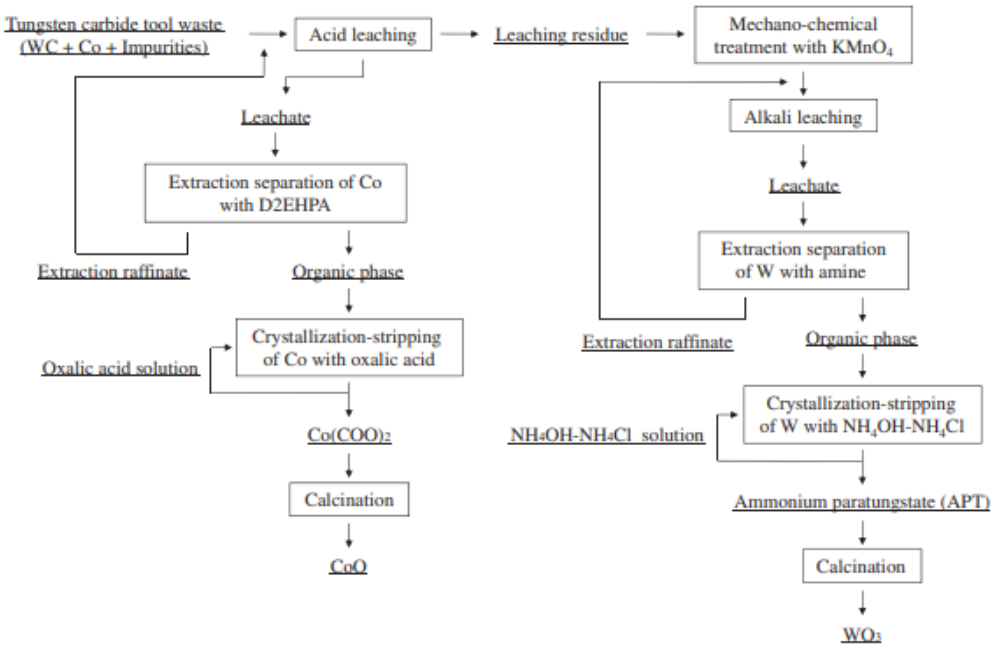

Figure 2.10. Hydrometallurgical recycling process for the recycling of tungsten carbide tool waste (Shibata *et al.*, 2012).

It is observed that acidic or alkaline leaching operations, in most hydrometallurgical techniques, are normally aided by mechanical (stirring, milling, etc.) or thermal (autoclaving) actions. This constitutes a disadvantage due to the consumption of huge amounts of energy plus the excess of chemicals needed to leach W from its ores, which makes these methods very expensive. The use of complexing agents for W (or Ca in the case of scheelite) allowed a substantial reduction in energy consumption (Guedes de Carvalho & Neves, 1992).

Due to the extremely high melting temperature of W, the hydrometallurgical process will continue to have a prevalence for W extraction from the tungsten ore concentrates. However, the new emerging technologies, such as electrochemical reduction of the tungsten ore, should be appraised by considering both the economic aspect of the process and the properties of the tungsten powder produced (Yang *et al.*, 2016). This know-how constituted a good point for the choice of electrolyte solutions and complexing agents, crucial in the electrochemical recycling processes presented below.

VI. Electrodissolution / Electrochemical process

Although the major recycling techniques are zinc process and cold stream process, electro-based technologies have been developed in parallel. In fact, recovering WC from cemented carbides by electrolysis had been used since the 1950s (Lin *et al.*, 1995).

Electrometallurgical ways of recycling WC scrap (electrochemical, electrodissolution, anodic dissolution, anodic-leaching/electro-leaching techniques, or electrowinning) consist in a one-step process and requires less energy, depending on the type of electrolytes used. Currently, electrodissolution techniques provide very pure results when compared with other WC-Co waste recycling methods (Katiyar & Randhawa, 2020).

The recycling of WC-Co waste is carried out through the electrodissolution process wherein the scraps of WC-Co act as an anode, and the graphite/stainless steel act as a cathode, with both anode and cathode being immersed into the electrolyte (acid/alkaline) during the electrochemical reaction. The distance between anode and cathode, as well as other electrochemical parameters, are optimized to reduce the energy consumption and increase cell efficiency, and the electrolytes can be regenerated and reused after some alterations (e.g. pH). An electrochemical reaction is triggered after a power supply is provided to the cell: the positive power supply is connected to the anode and the negative one to the cathode. Thus, after the anodic dissolution of the waste material starts, Co migrates to the solution and deposits on the cathode, and the remaining carbides break and fall to the bottom of the cell (Katiyar & Randhawa, 2020).

However, the anode passivation decreases the process efficiency and limits the electrodissolution, so improving the productivity of the anodic dissolution techniques remains a big concern for researchers. In addition to solving the problem related to passivation, researchers are involved in reducing the number of steps needed to reach the final product. In this context, various reagents (electrolytes) with different concentrations have been tested to develop a simpler and efficient process. Those are the acid-based reagent (HCl (Figure 2.11), HNO_3, H_2SO_4, and H_3PO_4) with low pH and the alkaline-based reagent (NaOH and NH_4OH) with high pH (Katiyar & Randhawa, 2020).

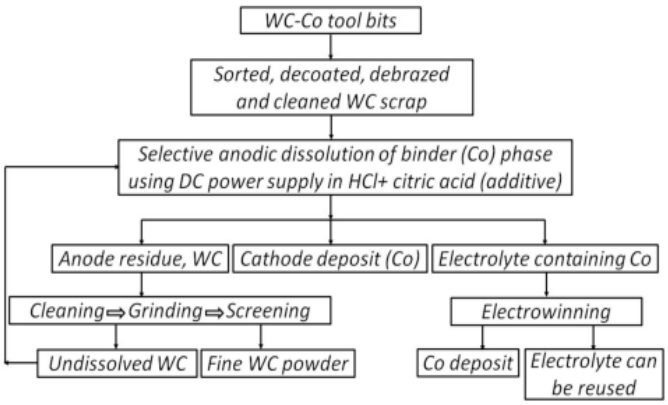

Figure 2.11. Process flow chart for the WC recycling using electrodissolution in acidic media (Katiyar & Randhawa, 2020).

Table A1 in the appendix resumes the several electrochemical processes for recycling WC waste (Katiyar & Randhawa, 2014). Initially, electrochemical technology has found some complex procedures and severe pollution, which have recently been overcome with new developments. The electrolysis method has many advantages like saving energy, almost zero pollution, high purity on the recovered product, and the equipment being relatively cheap (Lin *et al.*, 1995). However, this area is always in constant evolution. Below will be detailed some of the main advances in WC waste electrochemical recycling, using acidic electrolytes.

Nützel and Kuhl (1982) developed a method using nitric acid to dissolve the binder permitting at the same time the recovery of W compounds from the undissolved part of the hard metal. The binding metal is dissolved out of the scrap through electrolysis of diluted nitric acid solution between the scrap, serving as an anode and an inert cathode. According to these authors, the binding metal dissolution can be performed using diluted nitric acid (HNO_3) as the electrolyte at a higher rate than using HCl or H_2SO_4 electrolytes.

The undissolved part, mostly tungsten carbides, is transformed into tungsten oxides by heating above 700 °C until all the material has been oxidized. However, the heating of the hard metal under these conditions results only in very slow oxidation. This oxidized material is then dissolved in a sodium hydroxide solution and $NaWO_4$ is formed. Any components that are not dissolved in the sodium hydroxide solution can be separated after the clarified solution is acidified (e.g. with HCl). After acidification, yellow hydrated WO_3 precipitates and is separated by sedimentation or filtration, washed with diluted HNO_3, and dried at high temperatures. Thereafter, pure WO_3 is obtained without any traces of binding metal, so it can be reused by the industry for preparing new pure tungsten carbides (Nützel and Kuhl, 1982).

Madhavi Latha *et al.* (1989) also studied the influence of nitric acid on the Co dissolution and WC oxidation and diverse parameters of this system efficiency. The optimum conditions for simultaneous oxidation of WC and dissolution of Co are 10% HNO_3, a current density of 10 $kA/m^{2,}$ and a temperature of 55-60 °C. The oxidation of WC can be improved with the addition of dissolved Co, ammonium nitrate, or potassium perchlorate to the electrolytic solution. However, the Co deposition from a nitrate solution revealed a very low efficiency to be employed for the simultaneous deposition of dissolved Co at the cathode with oxidation of WC at the anode.

Lin *et al.* (1995) added citric acid to a 1-5 M HCl acid electrolyte in the electrolytic dissolution process as a means of avoiding the passivation of the rejected carbide waste at the anode. They are based on some authors' suggestions that the solubilization of scheelite and wolframite in citric acid solutions. The leaching of tungsten ores by inorganic acid (H_2SO_4 or HCl) solutions to which several organic anions (e.g. oxalates, acetates, etc.) have been added to help the dissolution by complex formation. It was also reported that oxalic acid provided higher W dissolution rates from scheelite (Guedes de Carvalho & Neves, 1992).

The inventors discovered that through the addition of a chelating agent, such as citric acid, to an acid electrolyte during selective electrolysis, the intermediate phase will undergo a complexing reaction at the anode. Citric acid, which influences the electrochemical treatment of WC-Co alloys had been studied for decades (see Hoar & Bucklow (1954)), is used as a chelating agent in electroplating baths for various W alloys (Zhang *et al.*, 2003), and seems an excellent option to prevent the formation of tungsten oxide on the outer surface of tungsten ores (Guedes de Carvalho & Neves, 1992).

Recently, the study of aqueous interactions between citric acid and tungsten (VI) revealed that a deficient amount of citric acid will result in the formation of insoluble tungsten oxides, because it may not form excess citrate acid as needed by the reaction mixture. The counter ion (e.g. Na^+) is essential to replace the hydrogen cations with sodium ones on citric acid and react with WO_4^{2-} to form tungsten citrate and balance the charge on the anionic complex (Zhang *et al.*, 2003). This is the principle behind the soluble tungsten complex that can be formed when citric acid is exposed to sodium tungstate (Na_2WO_4) and can be described by the following reaction (Llopis et al., 1993):

$$2WO_4^{2-}(aq) + 2Hcit^{3-}(aq) + 4H^+(aq) \rightarrow [W_2O_5(cit)_2]^{6-}(aq) + 3H_2O$$

This reaction allows tungsten to be solubilized, contrary to its normal tendency to form insoluble oxides, which allow the anode to dissolve freely. The authors conclude the addition of citric acid improved the ratio of Co dissolution from 49.4% to 80.7% and the dissolved W concentration from 9 mg/L to 536 mg/L, evidencing the significant influence of organic acids on the WC dissolution processes (Lin *et al.*, 1995).

In accordance with the high potential direct electrolysis method, tungsten carbide scrap serves as an anode and is electrolytically oxidized in tungstic acid slime. On the other hand, the Co cementing agent is dissolved in the electrolyte to form Co ions. The anode slime of tungstic acid is then recovered by extraction, or it is reduced to a W metal, while Co can be recovered by electrolysis or by precipitation with the addition of oxalic acid (Lin *et al.*, 1995).

1. Cobalt cementing agent phase:

$$Co\ (s) \rightarrow Co^{2+}(aq) + 2e^-$$

2. Tungsten carbide substrate phase:

Outer layer: $WC\ (s) + 2H_2O \rightarrow WO_2(aq) + 4H^+ + C + 4e^-$

Inner layer: WC is not reacted

3. Co-W-C intermediate phase:

$$Co\ (s) \rightarrow Co^{2+}(aq) + 2e^-$$

$$WC\ (s) + 2H_2(g) \rightarrow WO_2(aq) + 4H^+(ads) + C + 4e^-$$

$$2WO_2(aq) + H_2O \rightarrow W_2O_5(aq) + 2H^+ + 2e^-$$

$$W_2O_5(aq) + 2H_2O \rightarrow 2WO_3(aq) + 2H^+ + 2e^-$$

According to the above reactions, the Co-W-C intermediate phase reacts to form a passive film of tungsten oxides such as WO_2, W_2O_5, and WO_3 when the cobalt is electrolyzed and dissolved. Moreover, the reaction on the outer layer of the WC-Co substrate will form a passive film such as WO_2, which will hinder the dissolution of cobalt, affecting the electrolysis efficiency (Lin *et al.*, 1995).

Regarding the acidic electrolyte, although the concentration of the acid electrolyte can vary from 0.1 M to 5 M, HCl 1-3M seems to be a preferable condition. This concentration of HCl has revealed a better Co dissolution when compared to other electrolytes commonly used such as nitric acid (HNO_3), phosphoric acid (H_3PO_4), or sulfuric acid (H_2SO_4) (Lin *et al.*, 1995).

The chelating agent used was citric acid in a concentration of 40 g/L, although there are several examples of other chelating agents, such as ammonium chloride, glycine, oxalic acid, and ethylenediamine-N,N,N′,N′-tetrachloric acid (EDTA). According to the process of the invention, the potential and the electrolyte are determined in advance based on the test data obtained by applying anodic potentiodynamic polarization scanning on a WC working electrode. The potential must be kept constant during the whole electrolysis between 200 and 600 mV, preferably above 400 mV (Lin *et al.*, 1995).

VII. Molten salts electrolysis

Several studies were conducted in molten salts to prepare W from tungsten-containing compounds. Generally, tungsten carbide is used as a sacrificial anode, electrochemically dissolved in a molten salt (e.g. NaCl-KCl) to supply W ions, which were consequently discharged on the cathode and deposited as tungsten powders. This process required high temperatures (~750 °C) to separate and recycle elemental W and Co from WC–6% Co scrap in NaCl–KCl (Zhang *et al.*, 2017; Xi *et al.*, 2017).

Molten salts also use the mechanism of the ion-exchange treatment, through anion or cation-exchange resins. For example, to obtain an aqueous solution of $NH_4.2WO_4$, the WO_4^{2-} ions contained in the aqueous solution of Na_2WO_4 are adsorbed on the anion exchange resin and are eluted by ammonium salt (e.g. NH_4Cl). This method revealed an adsorption capacity of approximately three times as much tungsten as the conventional amount. Some problems with some side reactions have been identified, which resulted in the resin clogging, but these could be solved by keeping the aqueous solution basic (Yang *et al.*, 2016).

2.1.3.2. Sustainability of the tungsten carbide recycling industry

Research and forecasts show that WC scrap will continue to be an increasingly important source of raw material for the worldwide tungsten industry (Shemi *et al.*, 2018). Statistics indicate that the recovery of W and Co from WC scrap covers about 20% to 30% of the total supply, reducing the raw material cost by about 15% to 50% (Katiyar & Randhawa, 2020).

The substitution of tungsten-based cemented carbides appears to be technically possible but implies higher costs and a decrease in performance in some cases, as W has a very special performance and is most of the time the best choice of material. Furthermore, potential substitutes for cemented tungsten carbides include cemented carbides based on other CRMs, such as niobium or titanium carbide (also a CRM for EU and USGS). Ceramic-metallic composites also are studied, but technology is not competitive at the moment (EC, 2020a).

Energy efficiency is an important cost driver for any process, with a huge impact on the profit margins of a business operation, so the optimization of WC recovery considering the minimum energy costs is not an exception. A few decades ago, one of the great advantages of the zinc recycling process (a direct method) was that it consumed three times less energy for producing virgin WC than the indirect conversion methods (Lassner & Schubert, 1999). However, the high cost of energy in various countries has made the zinc process an energy-intensive and costly process considered unfavorable. The future trend of WC recycling will support the less energy-intensive recycling processes (Shemi *et al.*, 2018).

The pyrometallurgical processes have disadvantages like consumption of more energy, emission of toxic gases, causing pollution. The selective electrochemical process has some advantages over hydrometallurgical and pyrometallurgical processes such as lesser steps, higher efficiency, and lower costs of production. Electrodissolution processes are also considered suitable because of the advantages such as the high recovery of metals with good purity and low emission of harmful gases (Katiyar *et al.*, 2014).

Energy efficiency is not the only sustainability driver for WC recycling. The process cost includes the reagents cost, namely the adjuvants like inorganic and organic acids used in indirect methods; conversion costs related to the reinsertion of WC scrap in the recycling process itself; and the purity of scrap metal (Shemi *et al.*, 2018). All these factors, along with an environmental impact assessment and market availability and acceptability of the recycled product, will take part in a complete and necessary lifecycle assessment (LCA). Furberg *et al.* (2019) and Ma *et al.* (2017) did the first steps in that way. LCA is recommended not only to focus on WC production but also to compare other processes for recycling, especially for

chemical processes which found typical differences due to the many types of tungsten scrap available (Furberg *et al.*, 2019).

However, the recycling plants economy depends on the quantity and quality of the recovered products and the flexibility of the implemented process. Therefore, recycling industries play an essential role in the development of the WC market, whose advancement shows to achieve a negligible negative influence on the environment (Katiyar *et al.*, 2014; Katiyar & Randhawa, 2020). WC recycling industry joins the product manufacturers, the consumer industry, as well as the primary and secondary tungsten raw material producers. The balance between the primary and recycling sources leads to more predictability and stability in tungsten raw material costs, so investing in this relationship will help sustain and encourage the prospects of the WC recycling industry. This self-regulating balance brings a greater resilience to market fluctuations, benefiting all stakeholders: primary producers, product manufacturers, recycling companies, and clients. Companies like Sandvik (from Sweden) have had this type of balance successfully for decades (Shemi *et al.*, 2018).

A global perspective of the WC recycling industry, including future trends, is equally important to analyze the evolution of sustainability of the sector. As mentioned, world W supply is generally dominated by Chinese production and exports, with growing expectations for the coming years. The International Tungsten Industry Association (ITIA) related that China imposed stricter regulation and export taxes on the W industry. This is applied not only to primary tungsten mines and tungsten concentrates as a by-product from the mining of other metals, but also to tungsten by-products, such as tungsten carbide. It leads several companies to restart W mines or develop new W deposits in Europe, North America, Asia, and Australia, which can change the paradigm of the WC industry (EC, 2018; Shemi *et al.*, 2018).

2.2. Electrodialytic process

2.2.1. Principles

The electrodialytic (ED) process was developed at the Technical University of Denmark in 1992 and was patented in 1995 (PCT/DK95/00209). The ED remediation is a technique that relies on the application of a low-level direct current (DC) and combines the electrokinetic (EK) remediation method with electrodialysis. ED and EK are similar processes, except that ED uses ion exchange membranes to separate the contaminated matrix from the electrode compartments, while EK uses passive membranes. Ion-exchange membranes increase the removal efficiency due to the good conducting properties of the membranes, decreasing power consumption and providing good chemical stability over an extensive pH range (Ribeiro & Rodríguez-Maroto, 2006).

In practice, ED technology is an optimization of the EK process (Villen-Guzman *et al.*, 2019), which has been evolving to remove heavy metals not only from soils but from several environmental matrices, such as sludges, fly ashes, timber waste, and mine tailings (Ribeiro & Rodríguez-Maroto, 2006; Rojo & Hansen, 2006; Guedes *et al.*, 2014; Almeida *et al.*, 2020a).

In the ED process, one of the most important reactions that take place is water electrolysis (that will cause the pH changes), but several other reactions take place during the treatment. In an ED cell in which the matrix to be treated is placed in a suspension that is stirred, which is the case in this work, there are two main removal mechanisms: electromigration and electrodialysis. These reactions and mechanisms will be described in more detail below. Nonetheless, it should be referred that when the ED process is performed in a stationary system, there are other several transport mechanisms (similarly to EK), such as electroosmosis (the mass flow of pores in relation to soil particles under the influence of an electric potential gradient); electrophoresis (the movement of charged colloids under the application of an electric field); and diffusion (the movement of the species in areas under high chemical concentration gradients) (Ribeiro & Rodríguez-Maroto, 2006; Villen-Guzman *et al.*, 2019).

Reactions in the electrode compartments

Several interacting mechanisms make up the ED process, among which the dominant electron transfer reaction that takes place at electrodes is water electrolysis (Guedes *et al.*, 2014), which are represented in the following equations and Figure 2.12:

$$\textit{Anode: } 2H_2O \rightarrow O_2(g)\uparrow + 4H^+ + 4e^-$$

$$\textit{Cathode: } 4H_2O + 4e^- \rightarrow 2H_2(g)\uparrow + 4OH^-$$

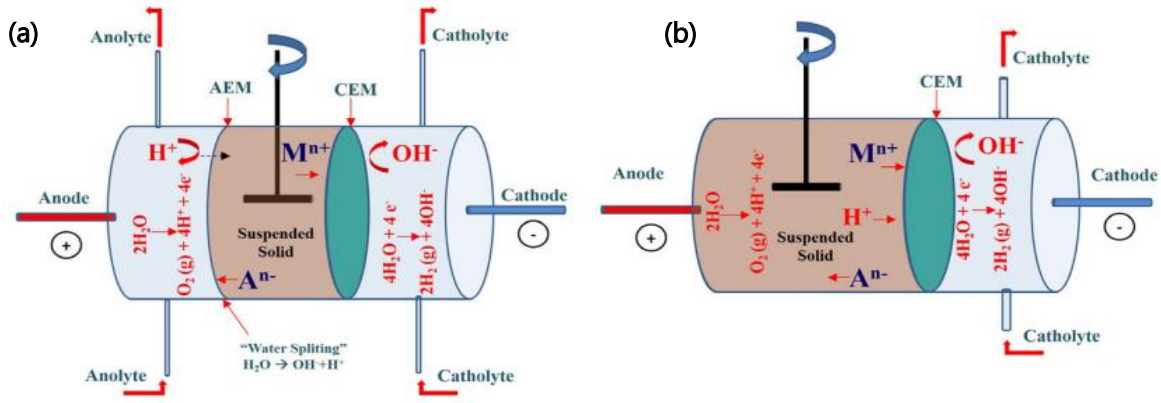

Figure 2.12. Schematic representation of a 3-compartment cell used for ED experiments applied to a stirred suspension of a solid matrix (a) *vs* 2-compartment cell (b) (Villen-Guzman *et al.*, 2019)

The electrodes must be inert to avoid reactions with metal-charged species present in the solution, so electrodes based on carbon, platinum, or titanium are usually used in the ED process (Nystrøm, 2001). The electric field generated by the applied current triggers the water electrolysis at the electrodes, inducing an alkaline media at the cathode and an acidic media at the anode. When the concentration of ions in the electrolytes increases, other electrode processes may take place at the surface of inert electrodes. The following equations are examples in which the Me^{n+} is a metal ion with *n* positive charges. The first equation represents the deposition of the metal at the cathode surface (Ribeiro & Rodríguez-Maroto, 2006):

$$\textit{Cathode: } Me^{n+} + ne^{-} \rightarrow Me$$

$$\textit{Cathode: } Me(OH)_n + ne^{-} \rightarrow Me + nOH^{-}$$

If chlorides occur in the solutions, chlorine gas can be also produced (Ribeiro & Rodríguez-Maroto, 2006):

$$\textit{Anode: } 2Cl^{-} \rightarrow Cl_2 \uparrow + 2e^{-}$$

In a basic 3-compartment (3C) ED cell, as represented in Figure 2.12a, ion-exchange membranes are used to separate the central compartment, where the contaminated matrix is placed, from the electrolytes. The anion exchange membrane (AEM) and cation exchange membrane (CEM) are used only allowing the passage of anions and cations, respectively. The electrodes are placed in the compartments at both ends where the electrolyte solutions circulate (Guedes *et al.*, 2014; Ribeiro & Rodríguez-Maroto, 2006). The dissociation of water molecules in the central compartment produces H^+ and OH^- to carry the electric current (water splitting), plus the proton leakage, both through the AEM, induces the acidification of the suspension. This acidic media increases the heavy metals removal during ED remediation (Kirkelund *et al.*, 2015; Villen-Guzman *et al.*, 2019).

In the 2-compartment (2C) cell, as represented in Figure 2.12b, the anodic solution can be placed together with the matrix suspension, combining the anolyte and suspension in a single compartment (PCT/EP2014/068956). This new design promotes more direct acidification of the suspension, where all H^+ ions produced by electrolysis at the anode will be supplied directly in the suspension. While in the 3C cell, the anions are removed to the anolyte and the oxidation of Cl^- ions to Cl_2 (g) occurs at the anode, in the 2C cell, faster oxidation and further removal is expected, since the electrode is in direct contact with the suspension. Instead, if the heavy metals are present as anions in the 2C cell, they will not be removed from the suspension (Kirkelund *et al.*, 2015).

Electromigration

Electromigration is the movement of ions under an applied electric field. This is the primary transport mechanism in soils for soluble charged species, such as metal cations, and the most important transport mechanism for ions in porous media. The positive ions move in direction of the anode, while the negative ions migrate to the cathode (Ribeiro & Rodríguez-Maroto, 2006).

The electromigration flux (J_m) is given by:

$$J_m = -u * c\phi_e$$

Where: u and c are respectively the ionic mobility and species concentration, and ϕ_e is the gradient of electric potential.

Basically, the current efficiency of electromigration of a specific ionic species is determined by the proportion of electrical charge carried by the species of interest, relative to the amount of charge carried by all charge species in solution (Ribeiro & Rodríguez-Maroto, 2006).

Electrodialysis

Electrodialysis is an electrochemical process in which electrically charged membranes and electrical potential difference are used to separate ionic species from aqueous solutions (Fidaleo & Moresi, 2005). This movement results from the presence of ion-exchange membranes, whose selective permeability increases the efficiency of species transport from the cathode or anode. The flux does not circulate between the two electrolytes and the matrix is continuously depleted of anions and cations until there are no more ions to be transported. The resistance will increase until a certain level and then become constant (Ribeiro *et al.*, 1999).

The transport of ions between the matrix and the electrolyte/electrode is controlled by ion-exchange membranes (the CEM and the AEM). The CEM acts as a "rectifier", allowing only the passage of cations, which should lead to greater transport efficiencies of heavy metals to the cathode. Thus, in a 3C cell, the CEM prevents the introduction of H^+ ions from the cathode to the matrix suspension. The AEM avoids the entry of protons from electrolysis reactions at the anode to the matrix suspension. However, as the AEM is not a 100% perfect rectifier, some hydrogen ions can migrate from the anode end towards the cathode end, passing through the middle compartment and lowering the pH (Pedersen *et al.*, 2017; Ribeiro *et al.*, 1999, Guedes *et al.*, 2014).

Concerning the key parameters for ED application to suspended solid matrices, pH is the one that more affects the efficiency of the results. The acidification is caused by (1) water electrolysis at the anode that generates H^+, and in a 3C-cell it can pass to some extent the AEM

membrane and by (2) the water splitting at the AEM. Some authors studied the influence of liquid:solid ratio and current density also on the water splitting, concluding that higher values of these parameters can lead to the current limiting at the CEM being exceeded. That would involve water splitting at the CEM and consequently OH^- entering the solid, hindering the remediation processes (Villen-Guzman *et al.*, 2019).

Membranes must have a high exchange capacity to maximize counter-ion fluxes and minimize electrical resistance, high selectivity for oppositely charged ions, and high permeability to save energy during the transportation (Ribeiro & Rodríguez-Maroto, 2006). ED cell can be designed to promote either acidic or alkaline conditions in the material, ensuring desorption and subsequent transport of metals and/or metal complexes to the oppositely charged electrode, although acidic electrodialysis is most commonly used (Pedersen *et al.*, 2017).

The advantage of this membrane-based separation process is that the ions only move in one way (i.e. out of the waste matrix chamber), which means no energy is wasted for transporting ions from the electrode chambers into the waste matrix chamber. However, a considerable amount of energy is consumed to generate the electric field and in the matrix suspension stirring. Energy use can have a huge impact on operating costs, strongly affecting the economic sustainability of metals recovery by the ED process (Oliveira *et al.*, 2019).

2.2.2. W and Co recovery through ED process

The application of ED for WC-Co treatment is a semi-direct method because there is a need to transform the supplied material to powder of the same composition (direct phase) before starting the electrochemical dissolution of one component while leaving the other phase intact (indirect phase).

As referred before, during anodic dissolution, tungstate anion (WO_4^{2-}) and cobalt cation ($Co^{2+,3+}$) are produced in the respective electrolytes (Katiyar & Randhawa, 2013). In anodic dissolution, the anode is usually sacrificed, whereas in our work this technique was not used. We submitted a WC-Co waste powder to an acid dissolution to facilitate the desorption of W and Co from tungsten carbide, followed by electromigration and electrodialysis to separate the Co from the W. However, in both cases, some Co is expected to be deposited on the cathode, while a certain amount of disintegrated tool matrix may remain at the bottom of the electrolytic cell, which can be undissolved WC that precipitates during the Co dissolution from tungsten carbide (Katiyar & Randhawa, 2013).

In addition to the very specific features of tungsten, this method is very challenging because of the different behavior of Co and W. According to the Pourbaix diagram for W

(Figure 2.2) and Co (Figure 2.6), one of the elements tends to precipitate in a pH where the other shows a good dissolution rate.

Almeida *et al.* (2020a) and Rosário (2018) studied the application of the ED process for W recovery from mine tailings, simultaneously with arsenic (As) removal in a 3C cell. Since the mine tailings were not treated, the matrix was much more complex than the WC carbide, the matrix targeted on this work. The initial results revealed some difficulties in W recovery due to the low migration rate of W to the electrolyte compartment, which could be increased using a 2C ED cell. However, when working with a different matrix it is necessary to analyze the Co and W behavior, thus we started with 3C cell.

2.3. Analytical techniques

2.3.1. Inductively coupled plasma-atomic emission spectroscopy (ICP-AES)

Inductively coupled plasma-atomic emission spectroscopy (ICP-AES) is an emission spectrophotometric technique, which principal characteristic is that each chemical element emits energy at specific wavelengths for its chemical character. The ICP-AES can determine the element composition by selecting a single wavelength for a given element, whose intensity of the energy emitted by the chosen wavelength is proportional to the amount (concentration) of that element in the analyzed sample. Note that ICP-AES analysis requires a sample to be in solution (Murray *et al.*, 2000).

3. MATERIALS AND METHODS

3.1. Chemicals and solvents

All chemicals were analytic grade: NaCl (MERCK), HNO_3 ≥ 65% (Sigma-Aldrich), HCl 36.5-38% (Scharlau), Citric acid 99% (Sigma-Aldrich), Oxalic acid ≥ 99% (Sigma). The water was deionized and purified with a Milli-Q plus system from Millipore (Bedford, MA, USA).

3.2. Initial characterization

WC-Co scrap powder was provided by ReCarb (Boston, MA, USA). This material was originally a part of cutting tools.

An initial characterization of the sample was carried out by SEM-EDS micrographs (at Instituto Superior Técnico, Lisbon) and XRF (at CENIMAT, FCT NOVA).

3.3. Desorption experiments

To determine the acid influence in W and Co desorption and to find the best electrolyte (acid mixture) for the ED experiments, the desorption tests were carried out in three sets.

First, 0.5 g of WC-Co waste was mixed with 25 mL of two mineral acids – HNO_3 and HCl – with different concentrations (0.5, 1.0, and 2.0 M) in a 100 mL Schott flask to assess the influence of a mineral acid on Co and W desorption. The mixture was placed in a mechanical stirrer for 4 h at 180 rpm, at room temperature. After, they were filtered by vacuum through glass-fiber filters of 0.7 μm, and W and Co were determined by ICP-AES analysis.

Once selected the best mineral acid concentration, the following step was to select the best type/concentration of organic acid. Thus, 0.5 g of WC-Co waste were mixed with 25 mL of different organic acids – citric acid and oxalic acid – in a 100 mL Schott flask, together with the selected mineral acid conditions (HCl 1.0 M). Then the mixture was placed in a mechanical

stirrer for 4 h at 180 rpm, at room temperature, filtered by 0.7 µm glass-fiber filters, and W and Co were determined by ICP-AES.

The last was to study the desorption as a function of time using the best acid conditions, HCl 1.0 M and citric acid 0.4 M. Thus, 36 Schott flasks were placed in a mechanical stirrer at 180 rpm and three replicates were collected at each time point 30, 60, 90, 120, 150, 180, 210, 240, 270, 300, 330 and 360 min. The samples were immediately filtered by 0.7 µm glass-fiber filters, and W and Co were determined by ICP-AES.

3.4. Electrodialytic experiments

ED laboratory cell

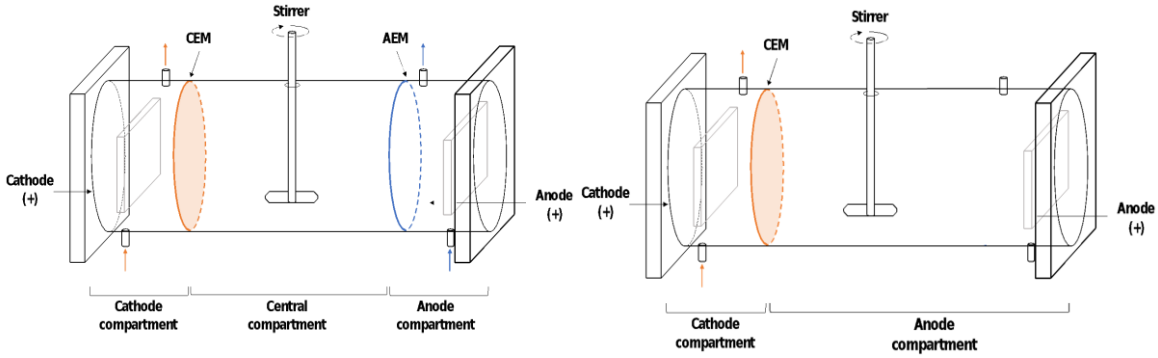

Figure 3.1. Configuration of (a) 3C ED cell and (b) 2C cell.

All experiments were carried out in ED modular reactors, that were assembled as either 3C or 2C cells (Figure 3.1. a) and b), respectively). All compartments have an internal diameter of 8 cm, a length of 10 cm in the sample (matrix) compartment, and a length of 5 cm in the electrolyte compartments. Commercial cation (CR67 MKIII blank; GE Water & Process Technologies) and anion exchange membranes (AR204R; Suez WTS Solutions USA) were also used to separate the compartments. The electrodes were made of mixed metal oxide (MMO), more specifically RuO_2–IrO_2/Ti (FORCE Technology, Brøndby, Denmark), and placed in the anode and cathode compartments. The WC-Co was treated as a suspension, in the central compartment of the 3C cell or anode compartment in the 2C cell, being constantly stirred by an overhead stirrer (VELP Scientifica Stirrer Type BS) at 250 rpm.

During the experiments, the electrolytes (catholyte and anolyte in the 3C cell, and catholyte in the 2C cell) had a constant recirculation ensured by a peristaltic pump (Watson-Marlow 503 U/R, Watson-Marlow Pumps Group, Falmouth, Cornwall, UK). A power supply E3612A (Hewlett Packard, Palo Alto, USA) was used to maintain a constant current in the ED cell, and the voltage was monitored in the same equipment. The pH of the catholyte was

manually adjusted to pH below 4 with 1:1 HCl when necessary. Figure 3.2 represents the setup of 3C ED experiments.

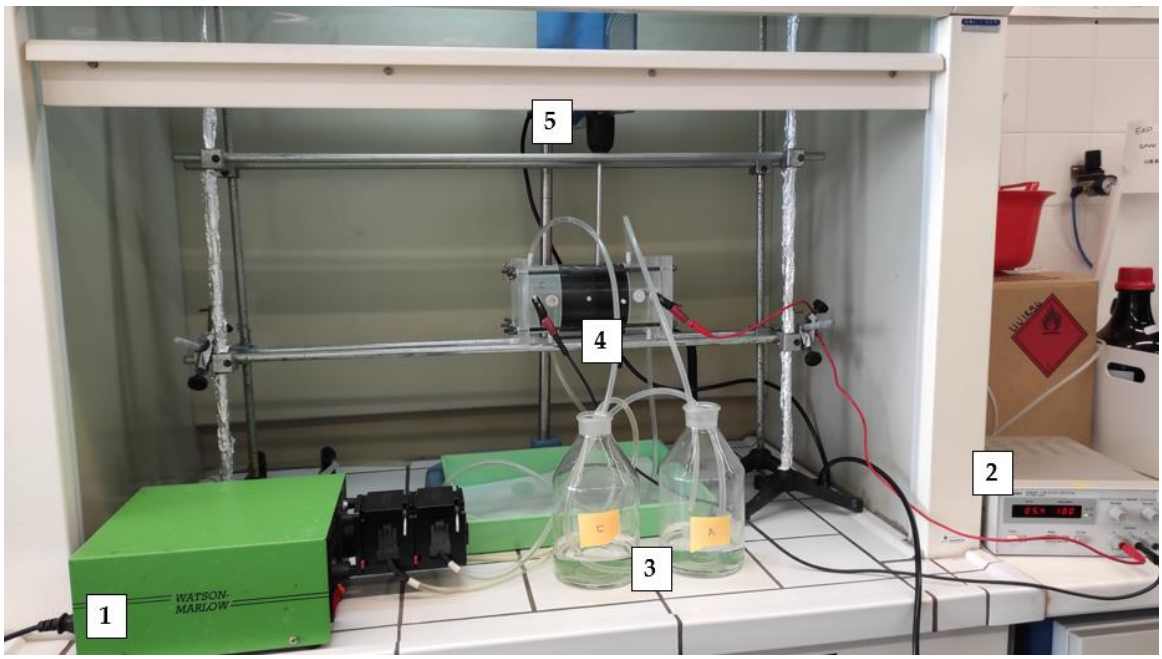

Legend: 1. Peristaltic pump; 2. Power supply; 3. Electrolyte bottles; 4. ED cell; 5. Stirrer

Figure 3.2. Experimental setup of 3C ED experiments. 2C cell setup was similar, except for the presence of anolyte and consequently the AN bottle.

Along with the experiments, the pH, conductivity, voltage drop, and current were monitored in the beginning, after approximately 5 h, and at the end of the experiments, 24 h.

At the end of all ED experiments, the sample suspension was recovered and filtered through 0.7 μm glass-fiber filters under vacuum, the volume was noted, and the solid was dried till constant weight. The electrolyte(s) were also collected and filtered through 0.7 μm glass-fiber filters under vacuum. The membranes and electrodes were embedded respectively in 50 mL and 40 mL of a mixture of HCl:Citric acid (1.0:0.4 M) for 24 h, to promote the W and Co dissolution. Then, the acid volume was filtrated through 0.7 μm glass-fiber filters under vacuum to remove eventual solid content. All liquid samples were sent for analysis in ICP-AES.

ED experiment conditions

ED experiments were carried out to perform three assessments (the best electrolyte, the best solid:liquid ratio, and the best current intensity), further described below and depicted in Table 3.1.

Table 3.1. ED experimental conditions.

Step	Exp. Code	Catholyte	Anolyte	Central compartment	Solid:liquid ratio	Current intensity (mA)
1 [a]	ED [NaCl]	NaCl	NaCl	NaCl	1:50	100
	ED [NaCl:HCit]			NaCl:Citric acid		
	ED [HCl:HCit]			HCl:Citric acid		
2 [b]	ED [1:75]	NaCl	Citric acid	-	1:75	
	ED [1:50]				1:50	
	ED [1:25] *				1:25	
3 [b]	ED [100 mA] *				1:25	100
	ED [150 mA]					150
	ED [200 mA]					200

Legend: [a] carried out with NaCl 0.2 M; [b] carried out with NaCl 0.02 M; * Same experiment, but different codes are used to simplify the discussion.
Note: HCl concentration was 1.0 M and citric acid (HCit) was 0.4 M.

Step 1: Assess the best acidic electrolyte

These experiments were carried out in a 3C cell, in which NaCl (0.2 M) was used as catholyte and anolyte. The WC-Co was placed in the central compartment and the supporting electrolyte was the variable: NaCl, NaCl:HCit, and HCl:HCit. All experiments were carried out with a solid:liquid ratio of 1:50 and a current of 100 mA.

Step 2: Assess the best solid:liquid ratio

These experiments were carried out in a 2C cell, in which NaCl (0.02 M) was used as the catholyte. The WC-Co was placed in the anode compartment and the supporting electrolyte was Citric acid. The variable was the solid:liquid ratio 1:75, 1:50, 1:25. All experiments were carried out with a current of 100 mA.

Step 3: Assess the best current intensity

These experiments were carried out in a 2C cell, in which NaCl (0.02 M) was used as the catholyte. The WC-Co was placed in the anode compartment and the supporting electrolyte was Citric acid, with a solid:liquid ratio of 1:25. The variable was the current intensity: 100, 150, and 200 mA.

3.5. Analytical methodologies

The ICP-AES analyses were carried out at the REQUIMTE laboratory in the Chemistry department of FCT NOVA.

3.6. Statistical analysis

Statistical analysis of the desorption tests was performed with GraphPad Prism software (version 9.2) to validate these results. The statistically significant differences between samples were assessed with a one-way ANOVA Tukey Test for a 95% level of significance. The statistically significant differences among Co and W were done for each element (between different concentrations in the same acid and between different acids for the same concentrations).

The ED experiments were not statistically analyzed because only one replicate of each experiment was carried out.

4. RESULTS AND DISCUSSION

4.1. Initial characterization

WC-Co waste powder was provided by ReCarb (Boston, MA, USA). This material was originally a part of cutting tools (Figure 4.1a) which were smashed to a powder (Figure 4.2b).

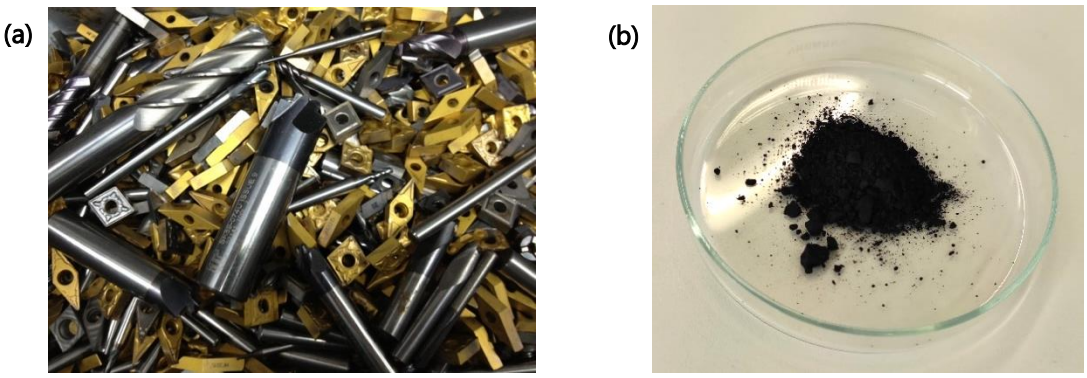

Figure 4.1. WC-Co scrap (a) and its resultant powder (b)

XRF (Table 4.1) and SEM-EDS (Figure 4.2) are different and semi-quantitative techniques, thus small differences in metals content values are expected. Furthermore, XRF does not quantify the carbon content. The elements concentration (mg/L) determination by ICP-AES analysis for the WC-Co scrap powder was not possible to attain during the execution of this work.

Table 4.1. Normalized percentage of elements (total identified 88.4%) determined by XRF for the WC-Co scrap powder. W and Co percentages are highlighted.

Element	**W**	**Co**	Ti	Ta	Nb	Fe	Cr	Mg
XRF Normalized concentration (%)	**89.2**	**6.76**	0.93	0.83	0.64	0.32	0.31	0.18
Element	Cu	Si	V	Ni	Ca	Zn	S	K
XRF Normalized concentration (%)	0.16	0.15	0.14	0.10	0.09	0.08	0.08	0.06

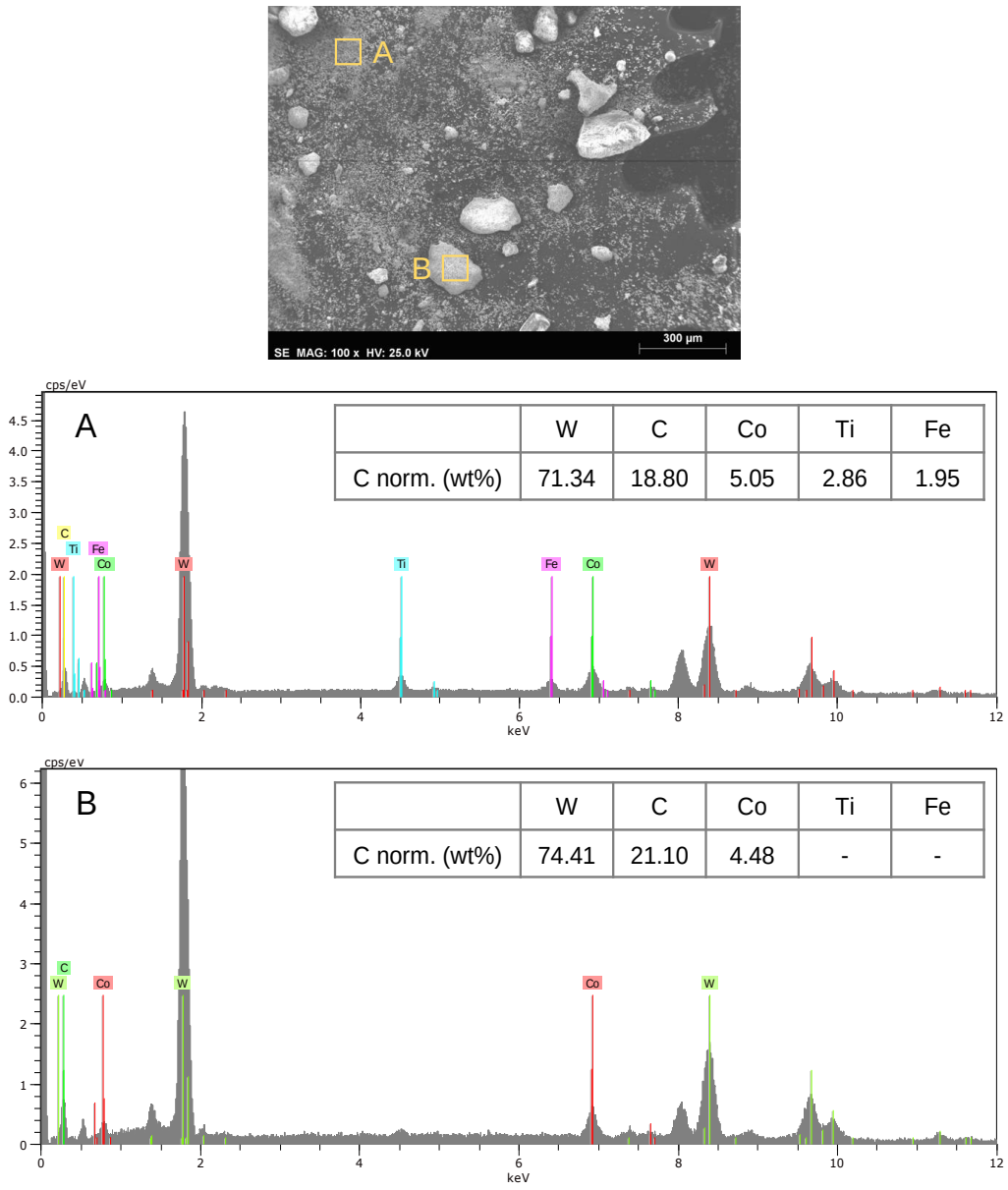

Figure 4.2. SEM-EDS micrographs of WC-Co scrap powder.

According to XRF, 6.8% of WC-Co is composed by Co, which agrees with the values mentioned in the literature review *(Chapter 2.1.3)* for tungsten carbide used in tools that require high hardness, used for metal cutting, mining, and wood working. In SEM, "phase" A corresponded to an analysis of the WC-Co smaller particle, while "phase" B focused on the analysis of a bigger particle region of the scrap. By observation of the SEM-EDS micrographs (Figure 4.2), the Co content in the WC-Co matrix (5%) is slightly below the normal content of Co (6%).

4.2. Desorption experiments

Tests were carried out to understand W and Co desorption from the WC-Co powder. The first test was performed to define the best mineral acid option. The HNO_3 has a great utilization in electrochemical recycling of WC-Co, as referred to in the literature review (*Chapter 2.1.3)*. However, HCl has also shown very interesting results in many studies *(Chapter 2.1.3)*. So, the comparison between these two mineral acids seemed pertinent.

After ICP analysis, the data treatment allowed us to conclude that the best mineral acid option is HCl at 1.0 M (Table 4.2). Although HNO_3 2.0 M shows the higher Co presence and one of the highest W values, there was a high standard deviation associated with it (relative standard deviation, RSD, of 88%), and therefore we opted for the HCl 1.0 M which reveals the highest W desorption with the lowest RSD (7%). Lin *et al.* (1995) also suggested HCl 1 M as a preferable condition.

Table 4.2. Concentration of Co and W desorbed according to the mineral acids' conditions tested (n=2). The selected mineral acid condition is highlighted.

Type and acid concentration	Co (mg/kg)	W (mg/kg)
HNO_3 [0.5 M]	12.2 ± 4.7	3.3 ± 1.7
HNO_3 [1.0 M]	14.9 ± 1.1	2.1 ± 0.3
HNO_3 [2.0 M]	14.6 ± 5.7	4.7 ± 4.2
HCl [0.5 M]	9.6 ± 4.7	3.1 ± 1.2
HCl [1.0 M]	10.1 ± 0.1	5.2 ± 0.4
HCl [2.0 M]	11.9 ± 2.3	2.4 ± 1.0

Citric acid ($C_6H_8O_7$) was proposed as a chelating agent by Lin *et al.* (1995) adding to HCl 1 M. As mentioned in *Chapter 2.1.3.*, it has been studied for WC-Co alloys treatment and reveals a good performance in ED remediation of mine tailings (Rojo & Hansen, 2006).

Oxalic acid ($C_2H_2O_4$) is another chelating acid, which revealed a good performance in hydrometallurgical processes, more precisely in the organic phase of leaching operations of Co (Shibata *et al*., 2012) but also in the W extraction in acid leaching (Guedes de Carvalho & Neves, 1992). Oxalic acid was also used as assisting agent in ED removal of heavy metals from timber waste (Ribeiro *et al*., 2000). Katiyar & Randhawa (2013) also compared the addition of these organic acids to an acidic electrolyte of HCl in potentiodynamic studies. Thus, the second test involves the testing of both organic acids, together with the selected mineral acid (HCl 1.0 M), to assess W and Co desorption.

The results obtained for the organic acids tests (Table 4.3) showed that there were no statistical differences between means except between citric acid 0.4 M and oxalic acid 0.4 M for Co. To better support the decision-making process, more replicates should be done. However, looking to Table 4.3, even with a high SD, citric acid 0.4 M has a much better recovery of Co than the oxalic acid 0.4 M, so citric acid 0.4 M was chosen and used in the subsequent experiments. Lin *et al.* (1995) also appointed citric acid as the best chelating agent, but in 40 g/L, equivalent to 0.2 M, while our results propose about twice that concentration, that is, 0.4 M citric acid, equivalent to 78 g/L. It should be referred that in Lin *et al.* (1995) the electrochemical system is different: the cemented carbide scrap (instead of powder) is placed in an anode basket and potentiostatic conditions (200-600 mV) were applied. These may explain the different results for the citric acid obtained here.

Table 4.3. Concentration of Co and W desorbed according to the organic acids' conditions tested in replicate (in an HCl 1.0 M solution; n=2). The selected organic acid condition is highlighted.

Type and acid concentration	Co (mg/kg)	W (mg/kg)
Citric acid [0.1 M]	11.1 ± 3.0	9.3 ± 2.6
Citric acid [0.2 M]	12.6 ± 0.7	14.4 ± 0.0
Citric acid [0.4 M]	18.1 ± 7.3	22.5 ± 6.7
Oxalic acid [0.1 M]	9.8 ± 1.0	15.2 ± 4.4
Oxalic acid [0.2 M]	3.8 ± 0.4	13.9 ± 1.7
Oxalic acid [0.4 M]	3.5 ± 0.0	19.3 ± 5.4

After selecting the best acidic conditions, desorption was carried out as a function of time. Analyzing the kinetic performance graph (Figure 4.3), Co has its highest desorption value (38 ± 1% mg/kg) approximately at 330 min since the stirring started, while W reached its highest value (59 ± 3% mg/kg) after 150 min. However, some values have a very high standard deviation (RSD above 39%). Still, it seems that a desorption plateau is achieved for Co after 200 min, whereas for W this was not observed.

The irregularity of kinetic performance for W values is well represented by Figure 4.3 and can be explained by several factors such as chemical behavior under acidic conditions but also sample heterogeneity: some heavier hard metal parts can still be found among the powder; and, as shown in the SEM micrographs (Figure 4.2), different particles sizes with different constituents' values can be found. Still, through simple sensible analysis, some outliers were identified and removed. Although this analysis had three replicates (n=3), the results suggest that in the future, the analysis should be performed again to increase the number of replicates, allowing a more robust statistical analysis to validate the results.

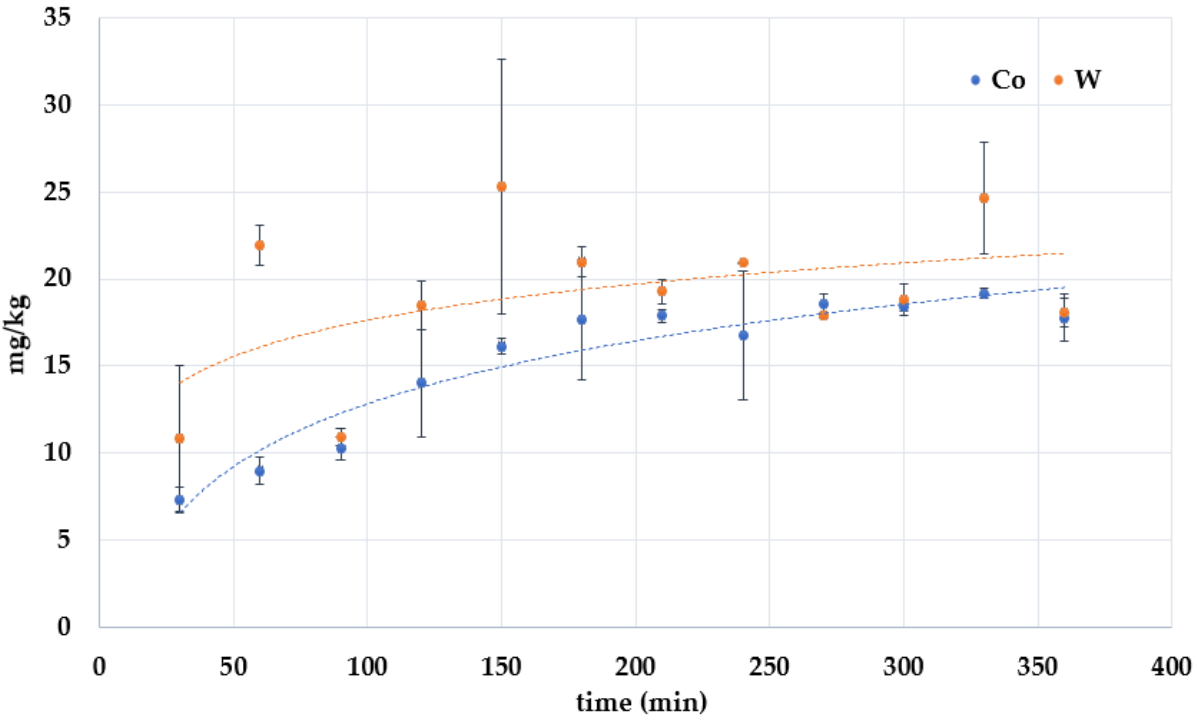

Figure 4.3. W and Co desorption as a function of time HCl:HCit (n=3).

4.3. Electrodialytic experiments

The ED experiments were carried out to assess the best parameters in three steps:

- Step 1: acidic electrolyte selection
- Step 2: solid:liquid ratio selection
- Step 3: current intensity selection

In all experiments, NaCl was used as an electrolyte, namely catholyte (in the 3C and 2C cell) and anolyte (in the 3C cell), as it has been claimed to be a suitable electrolyte on ED recovery by previous works (Gomes *et al.*, 2014).

4.3.1. Step 1 - Acidic electrolyte selection

In step one experiments, NaCl, NaCl:HCit, and HCl:HCit were added as electrolytes to the central compartment that contained the WC-Co aiming to enhance W and Co desorption and, consequently, electromigration. Table 4.4 shows the initial and final values for current intensity, the voltage drop between the working electrodes, pH, and conductivity.

Table 4.4. Initial and final values of ED control parameters on step 1 (3C).

Exp.	Current intensity (mA)	Voltage (V)	Catholyte		Anolyte		Central compartment	
			pH	Cond. (mS/cm)	pH	Cond. (mS/cm)	pH	Cond. (mS/cm)
ED [NaCl]	100 – 100	5.4 - 8.7	6.7 - 2.3	20.8 - 33.4	6.7 - 1.8	20.8 - 31.2	6.7 - 3.0	20.8 - 5.1
ED [NaCl: HCit]	100 – 100	5.3 - 6.3	6.2 - 4.4	20.5 - 27.7	6.2 - 1.5	20.5 - 38.2	1.8 - 2.5	23.7 - 5.8
ED [HCl: HCit]	100 – 100	4.5 - 3.8	6.5 - 1.7	20.1 - 31.9	6.5 - 1.5	20.1 - 40.3	1.0 - 1.5	100.4 - 24.2

It can be seen that conductivity increases in the anolyte and catholyte compartments as it decreases in the central one due to the ions migration towards the anode and cathode, which also causes the increase in the voltage. In the case of the cathode, the addition of HCl 50% to keep the pH around 4 also contributes to the increase in the conductivity of the catholyte. The catholyte pH control is an important variable as with an increasing pH there is a decrease of conductivity due to the precipitation of some elements, which increases the resistance and voltage, and consequently the electrical consumption (as schematized in Figure 4.4). Note that this sequence of relationships is applied to the catholyte of these experiments and occurred in all three steps of ED experiments.

Figure 4.4. Expected relations between pH and conductivity with electrical resistance at the catholyte.

In the ED [HCl:HCit], the initial and, consequently, final conductivity in the central compartment are much higher than in ED [NaCl] and ED [NaCl:HCit], which is reflected in a lower voltage. This is mostly attributed to the presence of HCl in ED [HCl:HCit] due to its higher concentration (HCl is 1.0 M contrary to NaCl 0.2 M and citric acid 0.4 M). Also, the presence of HCl may have contributed to a faster desorption of elements at the beginning of the ED experiment, thus contributing to an increase in conductivity.

The process of Co recovery has two parts: (i) the desorption of Co from the matrix (solid) to the acid mixture (liquid), followed by (ii) its electromigration as a cation to the catholyte. As it can be observed in Figure 4.5, ED [NaCl] and ED [NaCl:HCit] show a considerable migration of Co to the catholyte (CAT), while in ED [HCl:HCit], there is a lot of Co that remains in the central compartment (liquid phase). According to the Pourbaix diagram, the strong pink coloration in CAT [ED NaCl:HCit] (Figure 4.6a) corroborates this and alludes to

the presence of Co^{2+}. Figure 4.6b, namely the liquid phase (LP) (ED [HCl:HCit]), looks softer pink also because it is a less pure cobalt solution, as it is the liquid phase of the central compartment and there is a large presence of tungsten, but that allows to evidence the existence of Co.

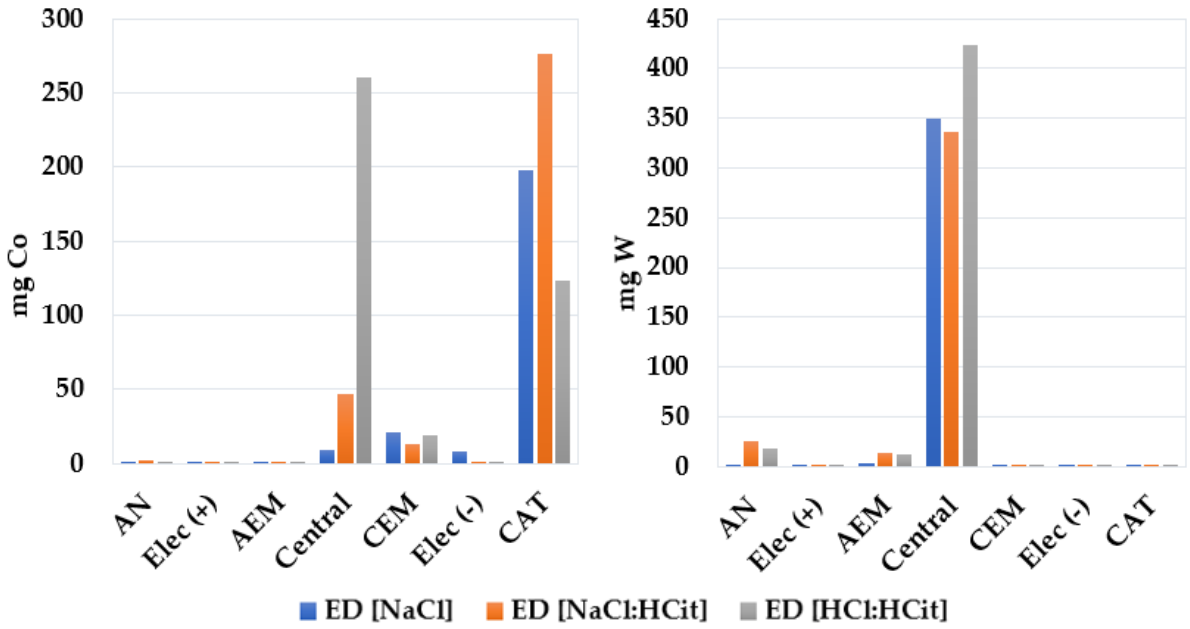

Figure 4.5. Mass of Co and W (mg) in each cell compartment in step 1 experiments. Note that the y-axis for Co and W are not at the same scale.

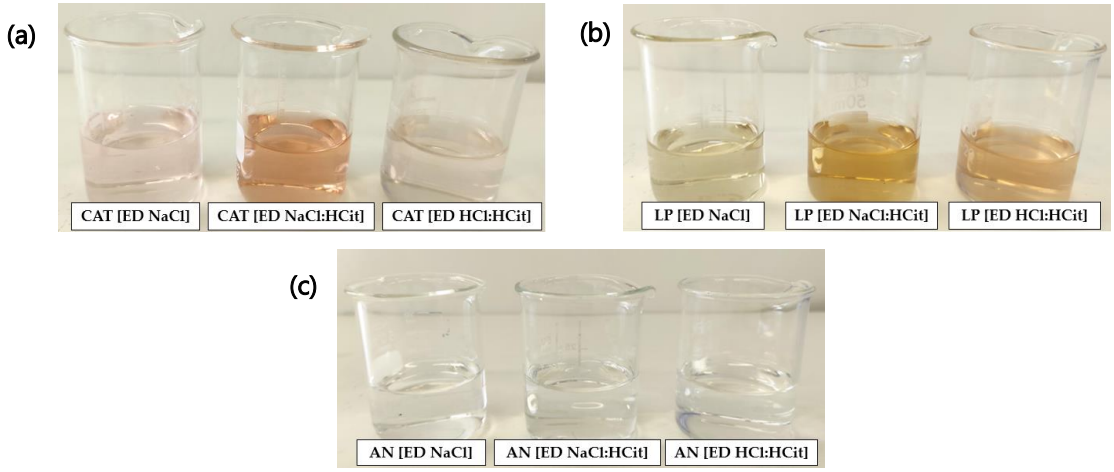

Figure 4.6. Catholyte (CAT) (a), central compartment (LP) (b), and anolyte (AN) at the end of step 1 experiments (after filtration).

The higher values of Co in the cathode side of ED [NaCl:HCit] show that NaCl:HCit as liquid phase in the central compartment promotes a good desorption and migration (~277 mg of Co in the catholyte). On the contrary, and although in ED [HCl:HCit] metal solubilization by the ED cell setup conditions is the highest one (~407 mg of Co *vs* ~238 and ~339 mg of Co

in ED [NaCl] and ED [NaCl:HCit], respectively), the migration of Co between compartments is not efficient (~261 mg of Co remains in the central compartment). The ions resulting from the dissociation of HCl, H^+ and Cl^-, can compete for the electromigration towards the cathode and anode. Thus, the high concentration of H^+ from the HCl may have hindered Co migration as the electromigration is not selective, i.e., all ionic forms can migrate. This is supported by the pH of the catholyte along the ED [HCl:HCit] that remained below 2, not being necessary to add HCl 50% in this experiment to control the pH, contrary to the observed in the other two experiments. To allow an efficient Co migration, perhaps it would be necessary to extend the time of the experiments. It should be noted that the presence of citric acid seems to slightly influence the amount of Co retained in the CEM (less ~8 mg of Co in ED [NaCl:HCit] than in ED [NaCl]).

Tungsten reaches the highest solubilization value ~458 mg (sum of W in all cell compartments) in ED [HCl:HCit] (Figure 4.5). But, in all experiments, a total of 98.5% in ED [NaCl], 89.1% in ED [NaCl:HCit], and 92.4% in ED [HCl:HCit] did not migrate from the central compartment, with a residual percentage being detected in the anolyte (Figure 4.6 c). This is attributed to the formation of neutrally charged W complexes. Although in ED [HCl:HCit], W reaches the highest solubilization value (~458 mg of W), the Co migration to the catholyte was very unsatisfactory when compared to ED [NaCl:HCit] (less 153 mg of Co in the CAT). This is an example of how W and Co have very different behaviors making the recovery of both these metals a challenge. Thus, considering both elements' behaviors, we chose to only use citric acid 0.4 M in step 2 experiments. The exclusion of NaCl from the mixture of the liquid phase aimed to save resources. Also, and considering that W does not migrate and that the anode compartment increases the process costs (price of AEM, the extra NaCl, and energetic costs due to anions (e.g. Cl^-) migration to the AN), in step 2 experiments we chose to change the 3 compartments cell (Figure 4.7a) to a 2-compartment cell (Figure 4.7b) to not only save resources and but also to increase the ED efficiency.

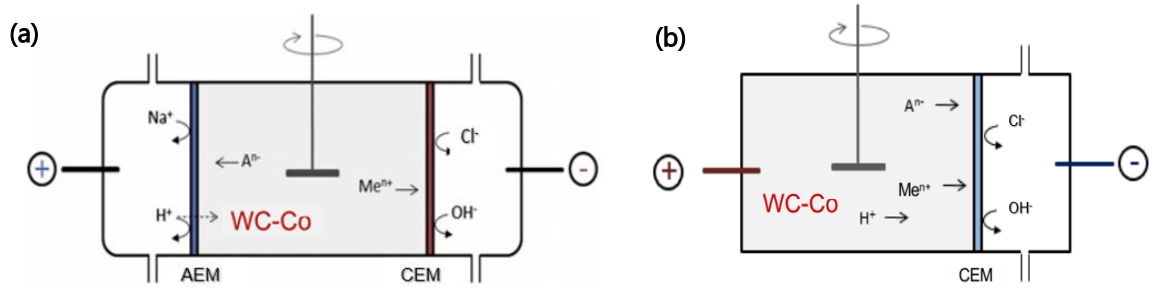

Figure 4.7. (a) Configuration of a 3C-electrodialytic stirrer cell (AEM: anion exchange membrane; CEM: cation exchange membrane); (b) Configuration of WC-Co in 2C cell.

The concentration of NaCl in the catholyte was also changed from step 1 to step 2 and 3 experiments from 0.2 M to 0.02 M, as there is a risk of a compensating reaction leading to

chlorine formation (Katiyar & Randhawa, 2013), the concentration decrease would decrease this risk, or the amount of chlorine potentially formed. This change was also performed considering that there would be no significant increase in the initial system voltage drop and consequently, the energy consumption.

4.3.2. Step 2 - Solid:liquid ratio selection

Step 2 aimed to assess the best solid:liquid ratio, 1:75, 1:50, and 1:25. The solid:liquid ratio is an important parameter aiming at preventing solution saturation and at finding the right balance between the amount of W that is released and forms complexes with the citric acid. If the concentration of citric acid is too low, most of the W will not form a soluble complex and will ultimately precipitate. In all three experiments of step 2, the final conductivity was lower (<10 mS/cm, Table 4.5) during the experiments than in step 1 ED [NaCl:HCit] experiment (>20 mS/cm, with the final conductivity in the central compartment, Table 4.4), which was reflected in a slightly higher voltage (around 8 V). This is explained by the lower NaCl concentration in the catholyte (0.02 *vs* 0.2 M) and its exclusion from the anolyte (liquid phase in step 1 experiment). Besides the reasons referred before for the use of a lower NaCl concentration, a lower concentration of NaCl also means a purer solution of Co in the catholyte as there is a lower impaction by Na^+ and Cl^-.

Table 4.5. Initial and final values of ED control parameters on step 2.

Experiment	Current intensity (mA)	Voltage (V)	Catholyte		Anolyte	
			pH	Cond. (mS/cm)	pH	Cond. (mS/cm)
ED [1:75]	100 – 100	13.0 - 8.4	6.7 - 2.4	2.3 - 7.8	2.2 - 2.2	6.0 - 7.7
ED [1:50]	100 – 100	9.4 - 8.2	6.6 - 3.8	2.8 - 3.6	2.2 - 2.1	6.2 - 8.2
ED [1:25]	100 - 100	10.5 - 7.5	6.6 - 3.9	2.5 - 5.3	2.3 - 2.2	5.8 - 9.3

Along with the experiments, and due to the increase in the catholyte pH to ~11, the cathode solution exhibited blue-green (Figure 4.8) shades. According to the Pourbaix diagram for Co (Figure 2.6), as the pH in the anolyte is ~2, Co should be present as Co^{2+}. As it migrates to the cathode side where OH^- is being formed due to the water electrolysis, it should yield the hydrated $Co(OH)_2$. As $Co(OH)_2$ is amphoteric, in an alkaline pH it yields the blue(-green) colored $HCoO_2^-$ (Schweitzer & Pesterfield, 2010). As the pH starts to decrease due to the addition of HCl to the catholyte, the previously blue-green solution begins to change to pink shades (Figure 4.8). According to the identified reactions and the Pourbaix diagram (Figure 2.6), Co^{2+} had been formed.

In Figure 4.8, it is possible to observe the moment when the reaction forms a thin line around the electrode in the middle of the compartment. The reaction appears to be dividing the cell into two different parts according to pH that is alkaline on the top and acidic closer to the bottom, where the electrolyte is entering with an acidic pH. Once the pH is homogeneous and ~4 in the cathode compartment, there is no longer pH shock between the anode and cathode sides, which decreases Co potential precipitation, that reduces the catholyte conductivity. It should be noted that a small amount of viscous blue-green cobalt was deposited at the cathode surface and close to the electrode, even after the pH reduction.

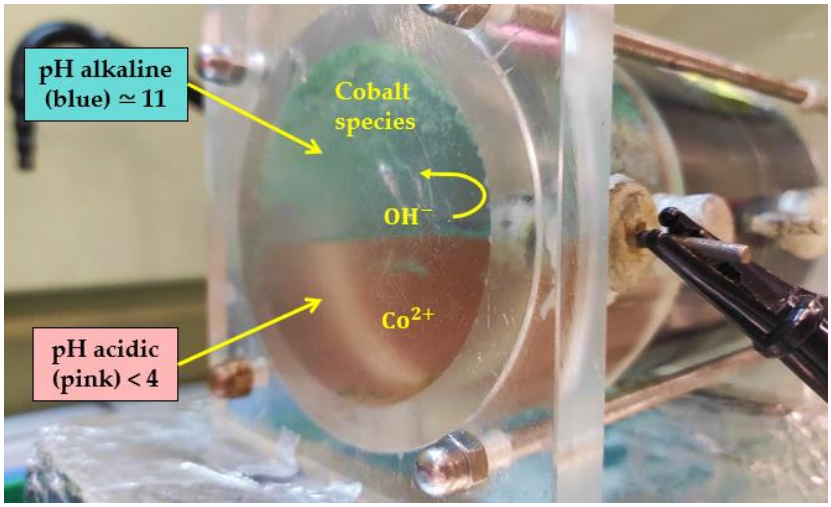

Figure 4.8. Co electromigration influenced by pH variation after HCl adding.

In Figure 4.9, it is clearly visible that experiment ED [1:25] has the best desorption values for Co (~732 mg of Co, summing the Co in all cell compartments) and W (~1413 mg). From this, 515 mg of Co were recovered in the catholyte (70.4% of the total Co solubilized), and 1408 mg of W remained in the anolyte (99.7% of the total W solubilized). From the remaining Co, 164 mg (22.4%) stays in the anolyte of the ED [1:25] and 49 mg in the CEM (6.7%).

As the pH in the catholyte is manually controlled, it changes from alkaline to acidic according to when the manual adjustment is done (e.g. pH is not controlled overnight, thus it increases to ~11). This high pH in the catholyte may have hindered the migration of Co from the membrane as it can clog the membrane due to the formation of $HCoO_2^-$ (the CEM becomes blue-green colored in the surface when the pH is not adjusted). A solution to this may pass through the installation of an automatic pH controller (more detailed in *Chapter 6. Future developments*), that could bring pH stability to ~4 and help to avoid Co precipitation in the CEM, thus increasing the efficiency of Co ions passage through the membrane. Also, as explained before, if the experiment was prolonged by 48 or 72h, the Co migration should increase. This prolongation in time could also elucidate whether the higher concentration of the sample in the ED [1:25] can result in a catholyte saturation and also hinder Co recovery.

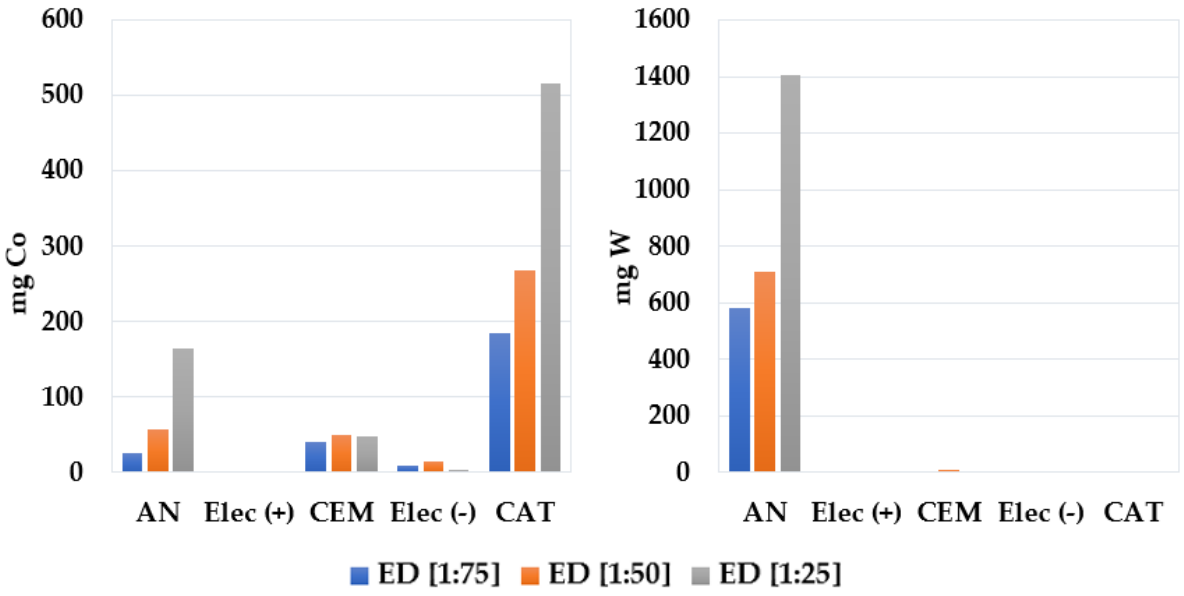

Figure 4.9. Mass of Co and W (mg) in each cell compartment in step 2 experiments. Note that the y-axis for Co and W are not at the same scale.

The good W recovery means that the alteration of the ED setup from 3C to 2C cell to increase the process efficiency was achieved (Figure 4.5 *vs* Figure 4.9). According to the literature, citric acid when exposed to W forms a soluble complex (Shemi *et al.*, 2018), and its concentrations increase as the WC-Co amount is increased in the cell. Thus, and attending to anolyte color (Figure 4.9), as the solid:liquid ratio is increased, the anolyte begins to gain darker tones which may be related to the increase in W concentration, 593, 722 and 1413 mg of W in ED [1:75], ED [1:50] and ED [1:75], respectively (Figure 4.8).

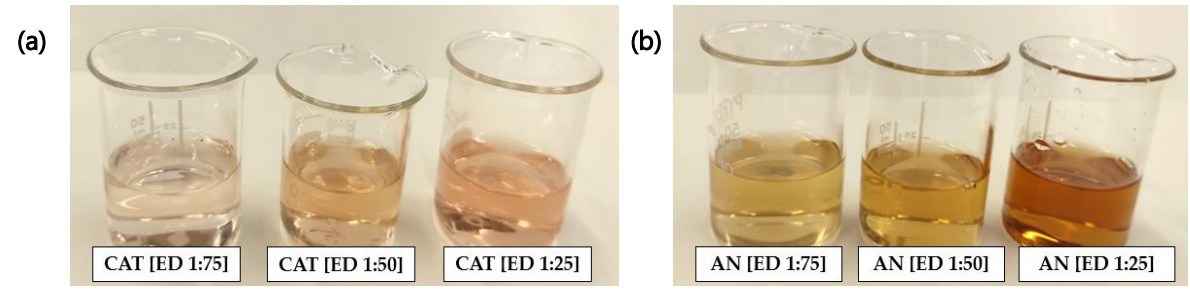

Figure 4.10. Catholyte (a) and anolyte (b) at the end of step 2 experiments (after filtration).

It is not possible to conclude what is the W species presents in the solutions. According to the Pourbaix diagram, the light-yellow shades at ED [1:75] could indicate the presence of $WO_3.2H_2O$ (s). However, the solutions of Figure 4.10 were filtered (0.7 μm), so they were retained with in solid. For this reason, the solid remaining in the filter will be considered after the final solid extraction to quantify the W and Co that were not solubilized.

Summing-up, and comparing all experiments in terms of W amount in the anolyte and Co amount that passes to the cathode, from the whole mass that desorbed by matrix, ED [1:25] gives the best results being the solid:liquid ratio selected for the following experiments.

4.3.3. Step 3 - Current intensity selection

As we concluded in step 2, ED [1:25] revealed the best solid:liquid ratio, so it was used as a reference for applying a current intensity of 100 (ED [1:25] ↔ ED [100 mA]), 150 and 200 mA. Initial and final control parameters are presented in Table 4.6.

Table 4.6. Initial and final values of ED control parameters on step 3.

Experiment	Current intensity (mA)	Voltage (V)	Catholyte		Anolyte	
			pH	Cond. (mS/cm)	pH	Cond. (mS/cm)
ED [100 mA]	100 - 100	10.5 - 7.5	6.6 - 3.9	2.5 - 5.3	2.3 - 2.2	5.8 - 9.3
ED [150 mA]	150 – 150	12.8 - 8.0	6.6 - 4.1	2.7 - 6.3	2.1 - 2.0	6.3 - 10.3
ED [200 mA]	200 – 170/180	16.1 - 83.0	6.6 - 3.4	2.7 - 5.7	2.1 - 1.9	6.3 - 12.5

In opposite to Lin *et al.* (1995), we worked under galvanostatic conditions (constant current), while they worked under potentiostatic conditions (constant voltage, potential). This is based on Ohm's law, if the current intensity *(I)* is constant, the voltage (*V)* decreases as the resistance also decreases:

$$I = \frac{V}{R}$$

Where: *I* - Current intensity (A/m²); *V* - Voltage (V); *R* - Resistance (Ω)

When conductivity increases in solutions, the resistance decreases and, consequently, the voltage decreases to maintain the same current. If the conductivity of the medium decreases, the resistance of the medium increases, so the voltage increases to keep the current constant. In our galvanostatic system, if the voltage reaches the maximum that the current generator used allows (equipment limit), the current intensity starts to decrease.

No major differences were observed in experiments conductivity, being only slightly higher at the end in ED [150 mA]. The pH was also similar between experiments. In terms of voltage, in ED [200 mA] a high increase in the voltage was observed, contrary to the other experiments in which the voltage remained low. In ED [200 mA] as the voltage reached ~83 V, the maximum allowed by the current generator, the current intensity started to decrease (as expected by Ohm's law), permanently oscillating between 170 to 180 mA. This means that the resistance of the system increased. As the conductivity of the anolyte and catholyte are

similar between the experiments (Table 4.6), the resistance increase was attributed to the electrode's stability. In fact, as it can be observed in Figure 4.11b, a color change in the anode of ED [200 mA] was observed which may mean that the electrode is being sacrificed.

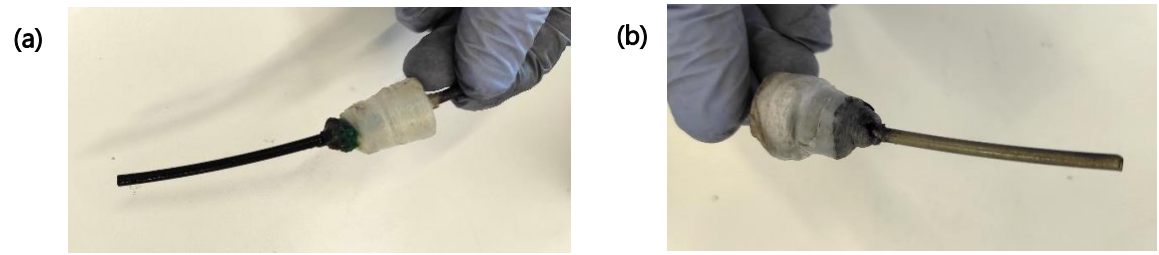

Figure 4.11. ED [200 mA] electrodes: (a) cathode, which did not react, and (b) anode less dark which indicates loss of stability.

The anode (positive electrode) in ED [200 mA] was sacrificed because the cell reached extreme conditions and lost stability increasing its resistance to the passage of current. The current began to decrease (from 200 mA; ending between 170-180 mA) and started to be converted into heat energy, resulting in the electrolyte heating up. This reflects in a higher temperature: the anolyte at ED [200 mA] surpassed 30 °C, whereas the other ED experiments remained at room temperature (23-24 °C). This effect is called Joule heating, where heat energy is being produced by the passage of an electrical current through a conductor:

$$P = IV$$

Where: P is the power, the energy per unit time (W); I is the current intensity (A); V is voltage (V).

With a direct current (DC), Joule heating is directly related to ohmic heating or resistive heating (referred to Ohm's law, mentioned above).

One option to assess the WC-Co recovery at higher current intensities is to redo the ED [200 mA] with the same electrode material but using new electrodes (the electrodes were reused between experiments) or use other types of electrodes. Another option, and as the final value of ED [200 mA] was oscillating between 170 and 180 mA, is to perform an experiment with a current intensity of 175 mA, aiming to assess if currents above 150 mA are doable.

Regarding metals recovery, Co desorption (total amount of Co in the ED cell) was higher in ED [100 mA] reaching ~732 mg of Co, followed by ED [200 mA] with ~687 mg of Co and ED [150 mA] with ~520 mg of Co. However higher recoveries in the catholyte were achieved in ED [200 mA] with 558 mg of Co and in ED [100 mA] with a slightly lower amount, ~515 mg of Co (Figure 4.12), all showing pink coloration (Figure 4.13a). The ED [150 mA] shows more less ~122 and 164 mg less of Co in the catholyte compared to ED [100 mA] and ED [200 mA],

respectively (Figure 4.12). When analyzing the final volume of the catholytes, ED [150 mA] shows a value below the others, and below the initial value (425 mL, less 75 mL than initial volume), attributed to a leak detected during the experiment. This loss may have resulted in the loss of Co during the experiment (the calculations were adjusted to the volume). For this reason, ED [150 mA] should be repeated to find out if the Co reduction is really caused by a possible leak or if the current is less efficient in extracting Co.

Nonetheless, a higher current, 200 mA, seems to improve Co desorption and its migration to the catholyte, with 81.3% of the total Co desorbed being detected in the catholyte, whereas for 100 mA only 70.4% of the total Co migrated to the catholyte. The membrane clogging continues to show up due to some Co being retained in it due to pH shift, as referred before. But, as mentioned in step 2, with a more stable pH control this could be minimized.

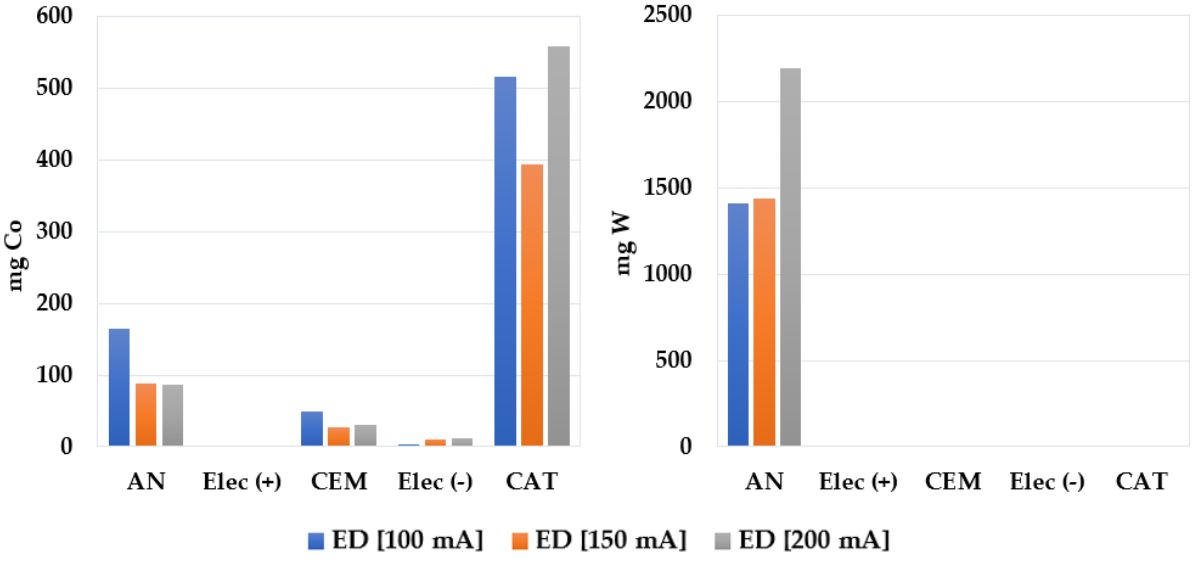

Figure 4.12. Mass of Co and W (mg) in each cell compartment in step 3 experiments. Note that the y-axis for Co and W are not at the same scale.

For W, a total of 2202 mg of W were desorbed from the WC-Co in the ED [200 mA], whereas the ED [100 mA] and ED [150 mA] presented less 788 or 764 mg of W, respectively. From the total W desorbed, ~99.6% (2194 mg of W) were present in the anolyte in all experiments. Looking at the final solutions of the anolytes in step 3 (Figure 4.13 b)), ED [150 mA] is lighter than the others. Following the same logic used in solid:liquid ratio assessment, a browner shade would be expected, compared to ED [100 mA] and considering that a higher current improves the desorption (considering the results for 200 mA). However, the W mass recovered is just 26 mg more than in ED [100 mA]. The application of a current intensity of 150 mA might not be enough to the W desorption or hydrated $WO_3.nH_2O$ could be starting to form.

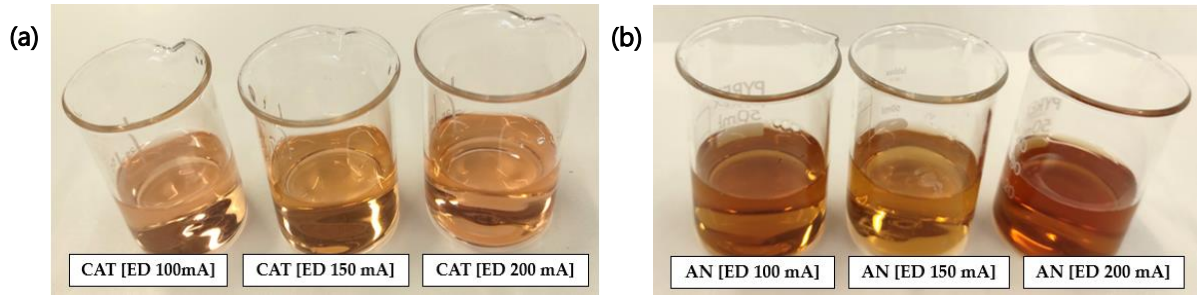

Figure 4.13. Catholyte (a) and anolyte (b) at the end of step 3 experiments (after filtration).

The anode solution of ED [200 mA] shows a different brownish shade (Figure 4.13 b)), a little closer to reddish. As mentioned before, brown color should be because of high concentration of W. This reddish color might indicate the presence of a different W complex compared to ED [100 mA] and ED [150 mA]. However, the reddish color obtained could also indicate a solution with lower W purity due to the electrode disintegration, for example. To test this, an ICP screening analysis could be performed to assess the presence of elements other than W and Co that might have resulted from the disintegrated electrode.

It should be mentioned that ED [200 mA] had a slight leak on the anolyte, thus the final volume was lower than the initial (400 mL, less 50 mL that initial anolyte volume). Perhaps if the ED cell were stable, the mass of W that we can desorb could be even higher, but only through a repetition, it can be proved.

Summing up, and despite the special conditions that occurred in ED [200 mA], this experiment presents promising values on metals recovery, both for cobalt and tungsten (Figure 4.12), with 558 mg of Co recovered in the catholyte and 2194 mg of W in the anolyte. Considering only W and Co, the anolyte is constituted by 3.8% of Co and 96.2% of W.

It seems that increasing the current intensity improves the migration of Co from the anolyte (AN) to the catholyte (CAT). Thus, it is important to define a current intensity that allows maintaining a low voltage to save energy while ensuring the best possible Co and W recovery. To reach the optimum conditions about current intensity, the following steps could be done:

- Redo the 150 mA experiment – due to the leak.
- Redo the 200 mA experiment with new mixed metal oxide (MMO) electrodes – MMO electrodes were reused between experiments.
- Perform an experiment with a current intensity of 175 mA – considering that the final voltage in ED [200 mA] oscillated between 170 and 180 mA to assess MMO electrodes stability.

- Test other electrodes aiming to increase the current intensity or check if other electrode materials would allow achieving higher recoveries at lower current intensities.
- After defining the optimum current intensity, a kinetic performance as a function of time (longer than 24 h, e.g. 72 h) should be done to assess the dynamic of Co electromigration and W desorption - this would allow us to understand the moment when the ED process reaches its efficiency limit.

As it was not possible to attain the analysis of WC-Co residues that remain in the cell after the application of the ED process, a small theoretical discussion will be performed considering W chemical behavior and the results obtained for the liquid phases.

Besides the complexes being formed with the citric acid, under acidic conditions tungstate ions should react with water electrolysis products and form hydrated tungsten trioxides (Nave & Kornev, 2016). Thus, the part of the W remaining in the solid phase after the ED process could be present as WO_3, a known product of the W recycling industry, even being commercialized. However, according to the Pourbaix diagram for W (Figure 2.2), the brown shades could also indicate WO_2, directly resultant of the reaction between tungsten carbide (WC) and water electrolysis, as one of the equations of the Co-W-C intermediate phase *(Chapter 2.1.3* (Lin *et al.*, 1995)*)*. Anyway, as mentioned in step 2, if the presence of W oxides (WO_3 or WO_2) was confirmed, that species were retained with the remaining solid after filtration.

As mentioned before, the electrodes are constituted by mixed metal oxides. However, some of these materials show limitations such as passivation, polarization, and corrosion. These processes may influence electrode stability, and consequently the ED process efficiency (as it happened in ED [200 mA]). However, it can be overcome by choosing the correct electrode materials and/or developing new electrode materials (preventing corrosion) and by powerful agitation of the electrolyte (preventing polarization and passivation) (Guedes *et al.*, 2021).

If there was passivation, this could be a barrier to the Co dissolution. Since the electromigration of Co to the catholyte seems satisfactory, the electrolysis may not be affecting the process too much and citric acid may perform its function to and prevent the passivation. The hypothesis that citric acid can form soluble tungsten complexes is not discarded (considering the values of W in the anolyte and its color). With a speciation analysis, both in liquid and the remaining solid, it will be possible to understand what W complexes were formed.

5. CONCLUSIONS

This is an innovative work, so the results obtained in this thesis are the preliminary part of a larger work. A successful treatment involving the W and Co recovery from industrial residues as a secondary source of critical raw materials will help to reduce the risk of supply disruption, both for the EU and the US considering their CRMs lists *(Chapter 2.1)*. The use of end-of-life cutting tools as a secondary resource can also prevent this material deposition in landfills as well as promote a circular economy chain.

Throughout all the work, there are many examples of how W and Co have different (electro)chemical behaviors. Co has a more predictable behavior, while W has a very irregular behavior, as shown by desorption as a function of time, and could be related with sample heterogeneity.

Right in step 1 of ED experiments, to assess the best electrolyte, W presented slightly better results in ED [HCl:HCit], but the use of HCl seemed to hinder Co migration and recovery to the cathode side. This reflects on how challenging it is to decide certain variables to ensure that the best possible choice for both W and Co recovery is found. For this reason, citric acid was used alone in the subsequent experiments in which the solid:liquid ratio (step 2) and current intensity were tested (step 3). Indeed, acidic conditions can facilitate the solubilization of WC-Co and, unlike other organic acids, citric acid is an environmentally friendly acid. The good performance of citric acid isolated (only adding HCl to stabilize the pH in the catholyte), reduces the risk of chloride formation, decreasing the production of Cl_2 which could be harmful.

In step 2, the solid:liquid ratio of 1:25 was chosen because it allowed recovering a significant mass of both metals, 515 mg of Co in the catholyte and 1408 mg of W in the anolyte. The percentage of W desorbed that migrates from the anode is residual, validating the efficiency of the 2C-cell reactor for the separation of Co from W.

Increasing the current intensity, step 3 tests, appears to improve the migration of Co from the anolyte (AN) to the catholyte (CAT): an application of a current intensity of 200 mA shows the highest recovery values for both Co and W, 558 mg (81.3% of the total Co solubilized) and 2194 mg (99.6% of the total W solubilized), respectively. However, as

mentioned before, due to extreme conditions that occurred particularly in this experiment, some new tests are recommended before the best current intensity condition can be defined.

In all cases, the membrane clogging, due to some Co being retained, may have influenced the Co recovered in the catholyte. For this, a more stable pH control should be performed or the experiment could be conducted for a longer time.

It should be mentioned that one constraint of this work was the impossibility of extracting the solid residue (WC-Co powder). The extraction and quantification through ICP-AES of W and Co remaining in the solid phase would have allowed to perform a mass balance of the entire process and more accurately assess the ED efficiency in the desorption and separation of W and Co. Also, replicates were not performed for the ED experiments. This was decided considering that this work was a preliminary assessment of the ED viability for W and Co recovery from WC-Co waste powder and, based on previous works, the replicability of the process concerning the recovery of heavy metals from mineral matrices is high. This decision also considered the time constraints that took into account the restrictions imposed by COVID-19, namely the restraints applied in March-April and the total occupancy of the laboratories. Nonetheless, and whenever possible, one replicate of each experiment should be done to support the conclusions of the ED process with statistical analysis.

Overall, the ED process showed to be a viable option for the separation and recovery of W and Co, and it should be further explored and optimized. This supports the viability of the ED technology for raw materials recovery, especially metals, from industrial residues. For example, and besides the work carried out in this thesis, there are other projects under development, e.g., to recover Co (and Li) from end-of-life batteries (Villen-Guzman *et al.*, 2019). The exchange of knowledge between works can be interesting and very important for improving the ED recovery of this critical element.

6. FUTURE DEVELOPMENTS

Future developments should consider the following (several already mentioned along with the discussion):

The extraction of the heavy metals content in the WC-Co solid residue before and after the ED process, followed by quantification by ICP-AES is very important, as mentioned before. Several efforts were carried out to extract W (the most difficult one) and Co using microwave digestion aiming to avoid the use of HF. For that, HNO_3 and HCl (isolated or as aqua regia) were tried together with different temperature runs but none was successful. So, HF combined with another acid (HF + HNO_3) or triacid attack (HNO_3 + $HClO_4$ + HF) will have to be used. This is currently being pursued.

After reaching the optimum conditions in terms of current intensity (mentioned in *Chapter 4.* in the discussion of results), a kinetic study as a function of time (longer than 24 h, e.g. 72 h) should be done in order to assess the dynamic of Co electromigration rate and W desorption.

The automation of a pH controller for ED experiments is under development at the RESOLUTION Lab, which will allow us to more accurately control the catholyte pH. It works by automatically measuring the pH of a solution and if the value is beyond a defined setpoint, the controller adds the acidic or basic solution to adjust the pH according to the defined setpoint. For example, in the ED recovery of W and Co, if we want a catholyte with pH < 4, when the pH of the catholyte exceeds this value, HCl will be automatically added. Thus, the ED cell gets more stability in pH, which could have a direct impact in avoiding the CEM clogging and improving the efficiency of Co^{2+} electromigration.

A spectrometric analysis should be done to analyze the speciation (in case of Co, to assess e.g. Co^{2+}; Co^{2+} complexes with Cl^-; while in W it should be mostly present as a neutral complex in the liquid phase or WO_3 or WO_2 in the solid phase). This know-how would allow us to better design the ED process by, e.g., controlling the reactions by controlling the system pH to avoid W precipitation. This would also allow assessing the viability of W recovered to be directly used by industry without further processing.

Another saline solution (e.g. $NaNO_3$) could be used as an electrolyte to avoid the use of NaCl, decreasing the risk of chlorides formation.

As mentioned in the introduction, to assess the effectiveness of the ED process for W and Co recovery, an economic analysis that includes the energy and material costs must be considered, and if it is possible with the inclusion of an LCA. This analysis was not done as the process is not yet optimized, but it is highly recommended that it is done when the optimum conditions are defined.

Assess the potential of the process to be coupled with a proton-exchange membrane fuel cell and determine its purity, as this could reduce the electrical energy requirements. According to *Chapter 2*, electrodeposition in aqueous solutions is an important process in the production of metallic W and Co. It has been reported that cobalt electrodeposition at pH < 4 occurs together with a hydrogen detachment reaction (Garcia *et al.*, 2008). Although in this work, the goal for Co was not the electrodeposition, but the desorption of Co followed by its electromigration to the cathode, the self-generation of H_2 in the cathode compartment is occurring in the ED experiments. This electrolytic hydrogen is mainly produced by water electrolysis, in addition to other cathode reactions (Magro *et al.*, 2019). One of the matrices tested was tungsten mine tailings (Almeida *et al.*, 2020b), presenting good H_2 production. As H_2 is a byproduct of self-energy generation (Magro *et al.*, 2019), it leads to considering the ED technologies as a potential hydrogen source and reducing its energy consumption. Still, after the process is optimized, all secondary reactions (anodic and cathodic) that may prevent or catalyze the formation of hydrogen must be evaluated. Later, a proton-exchange-membrane fuel cell could be attached to the catholyte to study the potential of this H_2 (including the purity of gas) to increase the energy efficiency of the ED treatment.

REFERENCES

Almeida, J.; Magro, C.; P. Mateus, E.; Ribeiro, A.B. (2021). *Life Cycle Assessment of Electrodialytic Technologies to Recover Raw Materials from Mine Tailings.* Sustainability 2021, 13, 3915. doi.org/10.3390/su13073915

Almeida, J.; Craveiro, R.; Faria, P.; Silva, A. S.; Mateus, E. P.; Barreiros, S.; Paiva, R.; Ribeiro, A. B. (2020a). *Electrodialytic removal of tungsten and arsenic from secondary mine resources — Deep eutectic solvents enhancement.* Science of The Total Environment, 710, 136364. doi:10.1016/j.scitotenv.2019.1363

Almeida, J.; Magro, C.; Mateus, E.P.; Ribeiro, A.B. (2020b). *Electrodialytic Hydrogen Production and Critical Raw Materials Recovery from Secondary Resources.* Water 2020, 12, 1262. doi.org/10.3390/w12051262

Alves Dias, P., Blagoeva, D., Pavel, C., Arvanitidis, N. (2018). *Cobalt: demand-supply balances in the transition to electric mobility.* EUR 29381 EN, Publications Office of the European Union, Luxembourg, ISBN 978-92-79-94311-9, doi:10.2760/97710, JRC112285.

Badawy, W. A., Al-Kharafi, F. M., & Al-Ajmi, J. R. (2000). *Electrochemical behaviour of cobalt in aqueous solutions of different pH.* Journal of Applied Electrochemistry, 30(6), 693–704. doi:10.1023/a:1003893122201

Cuesta-Lopez, S. (2017). Report on refractory metals increase potential-substitutes nonrefractory metals. Chapter 1. 4-15. MSP-REFRAM

Chen, T.-L., Kim, H., Pan, S.-Y., Tseng, P.-C., Lin, Y.-P., & Chiang, P.-C. (2020). *Implementation of green chemistry principles in circular economy system towards sustainable development goals: Challenges and perspectives.* Science of The Total Environment, 136998. doi:10.1016/j.scitotenv.2020.1369

European Commission (2020a). *Study on the EU's list of Critical Raw Materials, Factsheets on Critical Raw Materials.* ISBN 978-92-76-21049-8. doi: 10.2873/11619

European Commission (2020b). Critical Raw Materials Resilience: Charting a Path towards greater Security and Sustainability. Communication From the Commission to the European Parliament, the Council, the European Economic and Social Committee and the Committee of the Regions.

European Commission (2020c). *Critical materials for strategic technologies and sectors in the EU - a foresight study.* ISBN 978-92-76-15336-8 doi: 10.2873/58081

European Commission (2018). *Report on Critical Raw Materials in the Circular Economy.*

Falagán, C., Grail, B. M., & Johnson, D. B. (2017). *New approaches for extracting and recovering metals from mine tailings.* Minerals Engineering, 106, 71–78. doi:10.1016/j.mineng.2016.10.008

Fidaleo, M., Moresi, M. (2005). *Optimal strategy to model the electrodialytic recovery of a strong electrolyte.* Journal of Membrane Science, Volume 260, Issues 1–2, 90-111, ISSN 0376-7388. doi.org/10.1016/j.memsci.2005.01.048

Furberg, A., Arvidsson, R., Molander, S. (2019). *Environment life cycle assessment of cemented carbide (WC-Co) production.* Journal of Cleaner Production 209, 1126-1138. doi.org/10.1016/j.jclepro.2018.10.272

Garcia, E. M., Santos, J. S., Pereira, E. C., & Freitas, M. B. J. G. (2008). *Electrodeposition of cobalt from spent Li-ion battery cathodes by the electrochemistry quartz crystal microbalance technique.* Journal of Power Sources, 185(1), 549–553. doi:10.1016/j.jpowsour.2008.07.01

Godoy León, M. F., Blengini, G. A., & Dewulf, J. (2020). *Cobalt in end-of-life products in the EU, where does it end up? - The MaTrace approach.* Resources, Conservation and Recycling, 158, 104842. doi:10.1016/j.resconrec.2020.104842

Godoy León, M.F., Dewulf, J. (2020). *Data quality assessment framework for critical raw materials. The case of cobalt.* Resources, Conservation and Recycling, 157, 104564.

Gomes, H. I., Dias-Ferreira, C., Ottosen, L. M., & Ribeiro, A. B. (2014). *Electrodialytic remediation of polychlorinated biphenyls contaminated soil with iron nanoparticles and two different surfactants.* Journal of Colloid and Interface Science, 433, 189–195. doi:10.1016/j.jcis.2014.07.022

Guedes, P., Couto, N., Ottosen, L. M., & Ribeiro, A. B. (2014). *Phosphorus recovery from sewage sludge ash through an electrodialytic process.* Waste Management, 34: 886–892. doi.org/10.1016/j.wasman.2014.02.021

Guedes, P., Couto, N., Mateus, E. P., Pereira, C. S., & Ribeiro, A. B. (2021). *Perspectives on Electrokinetic Remediation of Contaminants of Emerging Concern in Soil.* Electrokinetic Remediation for Environmental Security and Sustainability, 18: 433–451. doi:10.1002/9781119670186.ch18

Guedes de Carvalho, R. A., & Neves, O. R. (1992). *Leaching of scheelite (CaWO4) under quasi-stagnant solution conditions.* Hydrometallurgy, 28(1), 45–64. doi:10.1016/0304-386x(92)90064-7

Hartmann, D., Yang Xiao, S., Casanovas, S., Garcia, R. B., Gonzalez Moya, M. (2016). Report on Current and Future Needs of Selected Refractory Metals in EU. MSP-REFRAM

Hoar, T. P., & Bucklow, I. A. (1954). *On the Electrodeposition of Tungsten-Cobalt Alloys From Aqueous Solutions.* Transactions of the IMF, 32(1), 186–210. doi:10.1080/00202967.1954.1186967

Jun, S. C., & Shinde, P. A. (2019). *Review on recent progress in the development of tungsten oxide-based electrodes for electrochemical energy storage. ChemSusChem.* doi:10.1002/cssc.201902071

Katiyar, P. K., & Randhawa, N. S. (2020). *A comprehensive review on recycling methods for cemented tungsten carbide scraps highlighting the electrochemical techniques.* International Journal of Refractory Metals and Hard Materials, 90, 105251. doi:10.1016/j.ijrmhm.2020.105251

Katiyar, P., Randhawa, N., Hait, J., Jana, R., Singh, K. & Mankhand, T. (2014). *An overview on different processes for recovery of valuable metals from tungsten carbide scrap.* Paper presented at: 18th International Conference on Nonferrous Minerals and Metals. ICNFMM;2014; Nagpur, At Nagpur.

Katiyar, P. K., Randhawa, N. S., Hait, J., Jana, R. K., Singh, K. K., & Mankhand, T. R. (2013). *Anodic Dissolution Behaviour of Tungsten Carbide Scraps in Ammoniacal Media. Advanced Materials Research, 828, 11–20.* doi:10.4028/www.scientific.net/AMR.828.11

Kirkelund, G. M., Magro, C., Guedes, P., Jensen, P. E., Ribeiro, A. B., & Ottosen, L. M. (2015). *Electrodialytic removal of heavy metals and chloride from municipal solid waste incineration fly ash and air pollution control residue in suspension – test of a new two compartment experimental cell.* Electrochimica Acta, 181, 73–81. doi:10.1016/j.electacta.2015.03.192

Lassner, E., & Schubert, W.-D. (1999). *Tungsten: Properties, Chemistry, Technology of the Element, Alloys, and Chemical Compounds.* Kluwer Academic/Plenum Publishers, New York. doi:10.1007/978-1-4615-4907-9

Leal-Ayala, D.R.; Allwood, J.M; Petavratzi, E.; T.J. Brown, T.J.; Gunn, G. (2015). *Mapping the global flow of tungsten to identify key material efficiency and supply security opportunities.* Resources, Conservation and Recycling 103.

Li, L., Ge, J., Wu, F., Chen, R., Chen, S., & Wu, B. (2010). *Recovery of cobalt and lithium from spent lithium ion batteries using organic citric acid as leachant. Journal of Hazardous Materials, 176(1-3), 288–293.* doi:10.1016/j.jhazmat.2009.11.026

Lin, J.C., Lin, J.Y., Lee, S.L. (1995). Process for Recovering Tungsten Carbide from Cemented Tungsten Carbide Scraps By Selective Electrolysis. US, Patent No. 5,384, 016.

Llopis, E., Ramírez, J. A., Doménech, A., & Cervilla, A. (1993). *Tungsten(VI) complexes with citric acid (H_4cit). Structural characterisation of $Na_6[\{WO_2(cit)\}_2O]\cdot 10H_2O$.* J. Chem. Soc., Dalton Trans., (7), 1121–1124. doi:10.1039/dt9930001121

Lunk, H.-J., & Hartl, H. (2019). *Discovery, properties and applications of tungsten and its inorganic compounds. ChemTexts, 5(3).* doi:10.1007/s40828-019-0088-1

Ma, X., Qi, C., Ye, L., Yang, D., & Hong, J. (2017). *Life cycle assessment of tungsten carbide powder production: A case study in China. Journal of Cleaner Production, 149, 936–944.* doi:10.1016/j.jclepro.2017.02.184

Madhavi Latha, T. & Venkatachalam, S. (1989). *Electrolytic recovery of tungsten and cobalt from tungsten carbide scrap.* Hydrometallurgy, 22(3), 353–361. doi:10.1016/0304-386x(89)90030-3

Magro, C., Almeida, J., Paz-Garcia, J. M., Mateus, E. P., & Ribeiro, A. B. (2019). *Exploring hydrogen production for self-energy generation in electroremediation: A proof of concept. Applied Energy, 255, 113839.* doi:10.1016/j.apenergy.2019.11383

Midwest Tungsten Service (2021). In https://www.tungsten.com/materials/tungsten/. Accessed July 25th, 2021

Murray, R.W., Miller, D.J., Kryc, K.A. (2000). Analysis of major and trace elements in rocks, sediments, and interstitial waters by inductively coupled plasma–atomic emission spectrometry (ICP-AES). ODP Tech. Note, 29

Nave, M. I. & Kornev, K. G. (2016). *Complexity of Products of Tungsten Corrosion: Comparison of the 3D Pourbaix Diagrams with the Experimental Data.* Metallurgical and Materials Transactions A, 48(3), 1414–1424. doi:10.1007/s11661-016-3888-6

Nystrøm, G. M. (2001). Investigations of soil solution during enhanced electrodialytic soil remediation. Master Thesis. Technical University of Denmark, Denmark.

Nützel, H.G. and Kuhl, R. (1982). Process for decomposing hard metal scrap. U.S. Patent 4-349-423.

Oliveira, V., Kirkelund, G. M., Horta, C., Labrincha, J., Dias-Ferreira, C. (2019). *Improving the energy efficiency of an electrodialytic process to extract phosphorus from municipal solid waste digestate through different strategies*. Applied Energy, 247, 182-189. doi:10.1016/j.apenergy.2019.03.175

Pedersen, K. B., Jensen, P. E., Ottosen, L. M., Evenset, A., Christensen, G. N., & Frantzen, M. (2017). *Metal speciation of historic and new copper mine tailings from Repparfjorden, Northern Norway, before and after acid, base and electrodialytic extraction.* Minerals Engineering, 107, 100–111. doi:10.1016/j.mineng.2016.10.009

Ribeiro, A. B. & Rodríguez-Maroto, J. M. (2006). Electroremediation of heavy metal-contaminated soils. Processes and applications. Cap. 18 In: M.N.V. Prasad, K.S. Sajwan, Ravi Naidu (Eds.), Trace Elements in the Environment: Biogeochemistry, Biotechnology and Bioremediation, Taylor & Francis, CRC Press, Florida, USA, ISBN: 1-56670-685-8, pp. 341-368.

Ribeiro, A. B., Réffega, A., Vieira e Silva, J. M., Villumsen, A. & Bech-Nielsen, G. (1999). O processo electrodialítico na remediação de solos contaminados por metais pesados. Actas da 6ª Conferência Nacional sobre a Qualidade do Ambiente, Lisboa, 20-22 October 1999, Vol. 2, pp. 773-782.

Ribeiro, A. B., Mateus, E. P., Ottosen, L. M., & Bech-Nielsen, G. (2000). *Electrodialytic Removal of Cu, Cr, and As from Chromated Copper Arsenate-Treated Timber Waste.* Environmental Science & Technology, 34(5), 784–788. doi:10.1021/es990442e

Rhodes, C. J. (2019). *Endangered elements, critical raw materials and conflict minerals. Science Progress, 003685041988487.* doi:10.1177/0036850419884873

Rizzo, A.; Goel, S.; Grilli, M. L.; Iglesias, R.; Jaworska, L.; Lapkovskis, V.; Novak, P.; Postolnyi, B.O.; Valerini, D. (2020). *The Critical Raw Materials in Cutting Tools for Machining Applications: A Review.* Materials 2020, 13, 1377. doi.org/10.3390/ma13061377

Rojo, A. & Hansen, H. K. (2005). *Electrodialytic Remediation of Copper Mine Tailings: Sulphuric and Citric Acid Addition. Separation Science and Technology, 40(9), 1947–1956.* doi:10.1081/ss-200054581

Rosário, A. (2018). Application of the electrodialytic process for tungsten recovery and arsenic removal from mine tailings. Master thesis in Environmental Engineering, Faculdade de Ciências e Tecnologia, Universidade Nova de Lisboa.

Schwertberger, D. (2016). Chemical behavior of tungsten in soils: Solubility, sorption and sequential fractionation. Master thesis. University of Natural Resources and Life Sciences Vienna, Austria

Seo, B. & Kim, S. (2016). *Cobalt extraction from tungsten carbide–cobalt (WC–Co) hard metal scraps using malic acid.* Int J Miner Process 2016; 151:1–7. doi:10.1016/j.minpro.2016.04.002

Schmidt, S., Geo, P., & Hutten, W. (2012). *From deposit to concentrate: The basics of tungsten mining Part 1: Project generation and project development.* International Tungsten Industry Association, 4: 1- 20.

Shemi, A., Magumise, A., Ndlovu, S., Sacks, N. (2018). *Recycling of tungsten carbide scrap metal: A review of recycling methods and future prospects.* Minerals Engineering, Volume 122, 195-205. doi.org/10.1016/j.mineng.2018.03.036.

Schweitzer, G. K. and Pesterfield, L. L. (2010). *The Aqueous Chemistry of the Elements.* Oxford University Press, Oxford.

Shibata, J., Murayama, N., Niinae, M., Furuyama, T. (2012). *Development of Adavanced Separation Technology of Rare Metals Using Extraction and Crystallization Stripping.* Materials Transactions, Vol. 53, No. 12, 2181-2186. The Japan Institute of Metals.

Slack, J.F., Kimball, B.E., & Shedd, K.B. (2017). Cobalt, chap. F of Schulz, K.J., DeYoung, J.H., Jr., Seal, R.R., II, and Bradley, D.C., eds., Critical mineral resources of the United States — Economic and environmental geology and prospects for future supply: U.S. Geological Survey Professional Paper 1802, p. F1–F40. doi.org/10.3133/pp1802F

Smol, M., Marcinek, P., Duda, J., & Szołdrowska, D. (2020). Importance of Sustainable Mineral Resource Management in Implementing the Circular Economy (CE) Model and the European Green Deal Strategy. *Resources*, *9*(5), 55. doi:10.3390/resources9050055

Sun, C., Xu, L., Chen, X., Qiu, T., & Zhou, T. (2017). *Sustainable recovery of valuable metals from spent lithium-ion batteries using DL-malic acid: Leaching and kinetics aspect. Waste Management & Research, 36(2), 113–120.* doi:10.1177/0734242x17744273

Tkaczyk, A. H., Bartl, A., Amato, A. Lapkovskis, V. & Petranikova, M. (2018). *Sustainability evaluation of essential critical raw materials: cobalt, niobium, tungsten and rare earth elements*. Journal of Physics D: Applied Physics, 51 203001.

United States Geological Survey (2018). Interior Releases 2018's Final List of 35 Minerals Deemed Critical to U.S. National Security and the Economy. In https://www.usgs.gov/news/interior-releases-2018-s-final-list-35-minerals-deemed-critical-us-national-security-and. Accessed in May 2021

Velenturf, A. P. M., Archer, S. A., Gomes, H. I., Christgen, B., Lag-Brotons, A. J., & Purnell, P. (2019). *Circular economy and the matter of integrated resources. Science of The Total Environment.* doi:10.1016/j.scitotenv.2019.06.449

Villen-Guzman, M., Arhoun, B., Vereda-Alonso, C., Gomez-Lahoz, C., Rodriguez-Maroto, J. M., & Paz-Garcia, J. M. (2019). *Electrodialytic processes in solid matrices. New insights into batteries recycling. A review.* Journal of Chemical Technology & Biotechnology. doi:10.1002/jctb.5940

Yang, J., Bourgeois, F., Bru, K., Hakkinen, A., Andreiadis, E., Meyer, D., … Yang, Y. (2016). State of the art on the recovery of refractory metals from primary resources. MSP-REFRAM, D2.2(688993), 112.

Wainer, E. (1956). Process for recovery of tungsten values. U.S. Patent No. 2735748

Xi, X., Xiao, X., Nie, Z., Zhang, L., & Ma, L. (2017). *Electrolytic separation of cobalt and tungsten from cemented carbide scrap and the electrochemical behavior of metal ions.* Journal of Electroanalytical Chemistry, 794, 254–263. doi:10.1016/j.jelechem.2017.04.001

Yildiz, Y. (2017). *General Aspects of the Cobalt Chemistry.* Chapter 1. In: Cobalt. Khan Maaz (Ed.), InTech, Rijeka, Croatia. doi:10.5772/intechopen.71089

Zhang, L., Nie, Z., Xi, X., Ma, L., Xiao, X., & Li, M. (2017). *Electrochemical Dissolution of Tungsten Carbide in NaCl-KCl-Na2WO4 Molten Salt. Metallurgical and Materials Transactions B, 49(1), 334–340.* doi:10.1007/s11663-017-1125-3

Zhang, H., Zhao, H., Jiang, Y.-Q., Hou, S.-Y., Zhou, Z.-H., & Wan, H.-L. (2003). *pH- and mol-ratio dependent tungsten(VI)–citrate speciation from aqueous solutions: syntheses, spectroscopic properties and crystal structures.* Inorganica Chimica Acta, 351, 311–318. doi:10.1016/s0020-1693(03)00177-4

A. APPENDIX

Table A1. Electrochemical recycling of W based scraps (adapted from Katiyar & Randhawa, 2020; references are included inside the article)

Tungsten-containing scraps	Electrolyte/ Additive	Current density	Recover product	Ref.
Tungsten alloy swarf (88% W, 7.5% Ni, 4% Fe, 0.3% Mo)	NaOH/ NaCl	0.2 A cm^{-2}	Ammonium paratungstate (APT)	Hairunnisha *et al.* (2007)
WC-6% Co	1.25 M H_3PO_4	-	Separation of Co from WC phase	Malyshev *et al.* (2004)
Cemented tungsten scraps	1-3 HCl/Citric acid	-	Separation of Co from WC phase and WC powder recovery	Lin *et al.* (1995)
Tungsten alloy swarf (96% W, 3% Fe, 1% Ni)	NaOH	-	W after chemical treatment	Srinivasan *et al.* (1994)
WC-Ni pseudo alloy (86.4% W, 5.8% C, 7.2% Ni)	H_2SO_4	2.50-4.50 A cm^{-2}	Tungsten oxide (WO_3)	Kuntyi *et al.* (2012)
WC-6% Co alloy	1.2 M H_3PO_4	1.5-3.0 A cm^{-2}	Cathode deposited Co and W recover after chemical treatment	Ghandehari *et al.* (1982)
Cemented tungstate carbide	NH_4OH	-	APT	Vanderpool (1991)
Sintered metal carbide scrap	NaOH	-	Disintegrate WC powder and Co deposited on the cathode	Vanderpool (1991)
WC-6% Co alloy	H_3PO_4	1-3-2.1 mA cm^{-2}	Separation of Co and WC phase	Malyshev *et al.* (2007)
Cemented carbide WC-87%, Co-13%	HNO_3	-	Cathode deposited Co and W after chemical treatment	M. Latha *et al.* (1989)
Tungsten	NaOH	2.74 A cm^{-2}	Tungstate solution	Davydov *et al.* (1997)

Tungsten-containing scraps	Electrolyte/ Additive	Current density	Recover product	Ref.
Secondary hard metal alloys	HNO_3	0.35-1.77 A cm^{-2}	WO_3	Zaichenko *et al.* (2010)
Sintered metal carbide scraps	HNO_3	-	Cathode deposited Co and W recover after chemical treatment	Kobayakawa (1979)
Heavy metal scraps	NH_4OH/ NH_4NO_3	-	APT	Vanderpool (1981)
Hard metal content 15% Co	HCl	-	Cathode deposited Co and W recover after chemical treatment	Yang *et al.* (2011)

2021

DAVID EMANUEL PINTO GASPAR

ELECTRODIALYTIC RECOVERY OF TUNGSTEN AND COBALT FROM AN INDUSTRIAL RESIDUE - PRELIMINARY ASSESSMENT

NOVA SCHOOL OF SCIENCE & TECHNOLOGY